

THE REDUCTION OF MASUKU CASSITERITE  
CONCENTRATE BY CHARCOAL AND CARBON  
MONOXIDE

By

Ralton Latoni Nyirenda

A dissertation submitted to the University  
of Zambia in partial fulfilment of the  
requirements of the degree of Master of Mineral  
Sciences in Metallurgy and Mineral Processing.

THE UNIVERSITY OF ZAMBIA

LUSAKA

1986

### DECLARATION

This report is an account of research conducted by R.L. Nyirenda in the laboratories of the school of Mines, UNZA, and the researcher attests that it is not a reproduction of work that has been submitted before for a degree at this, or any other University.

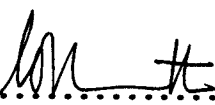
*R.L. Nyirenda*  
.....

R.L. Nyirenda

20th January, 1986

APPROVAL

This dissertation of Ralton Latoni Nyirenda is approved as fulfilling part of the requirements for the award of the degree of Master of Mineral Sciences in Metallurgy and Mineral Processing by the University of Zambia.

Signed .....  ..... Date. March 12, 1986  
Dr. A.E. Wraith

Signed .....  ..... Date. October, 17 - 1986  
Dr. J. B. Mwalula

Signed .....  ..... Date. 21-10-1986  
Dr. R. T. Shabana

### ABSTRACT

The reduction of Masuku Cassiterite gravity concentrate by charcoal was investigated in the temperature range of 850 to 1100°C. A combination of sample weight loss measurements, exit gas analysis and chemical analysis of the reaction products was used to monitor the course of the reaction.

The influence of temperature, charge porosity, relative amount of reactants and their particle size on the reduction rate was studied. Also considered was the effect on the nature of the reduction caused by lime addition to the charge.

It was found that the cassiterite could be best reduced by a combination of high temperature, reasonably high charcoal proportions, high charge porosity and the addition of a small percentage of lime.

Based on the assumption the rate controlling step was the reaction of carbon dioxide on the carbon surface, the kinetic data obtained from isothermal experiments was analysed and found consistent with the supposition. An activation energy of 60.8 kilocalories per mole was determined for the consumption of carbon by reaction with cassiterite.

Associated with the main investigation were other experiments designed to provide supplementary information on the  $\text{SnO}_2$  + carbon reaction. These experiments involved the reduction of cassiterite by carbon monoxide in the temperature interval of 900 to 1100°C.

The initial stages of the  $\text{SnO}_2 + \text{CO}$  reaction were studied by means of changes in pH of a KOH absorbent solution into which the product gas was dissolved. Additional data was derived from sample weight loss determination at the end of the experiment, and chemical analysis of the reaction product.

The prominence of the Boudouard reaction in the  $\text{SnO}_2 +$  carbon reaction process was brought to light by these latter experiments. An activation energy of about 35.6 kilocalories per mole tin produced, was found for the  $\text{SnO}_2 + \text{CO}$  reaction.

## A C K N O W L E D G E M E N T S

It is with great pleasure that I wish to express my gratitude to the following persons:-

Mr. J.W. van Poppelen, for assistance with XRF analysis of the concentrates and advice on much of the procedural aspects of the experiments.

Mr. J. Castel, for advice and help in setting up of the apparatus.

Professor A.M. Radwan, for having taken up much of his time in supervising the work at all stages.

Mrs. M. Sanga, for typing the manuscript and friends too numerous to name, for their very useful comments on many aspects of the research.

Errors of whatever kind which may have occurred, rest however, entirely upon me.

**R. L Nyirenda**

## CONTENTS

PAGE

## CHAPTER ONE: GENERAL SECTION

1. Introduction.....	1
2. The source and analysis of cassiterite concentrate...	3
3. Theory: (A) thermodynamics.....	6
(B) effect of temperature on kinetics.....	12

## CHAPTER TWO: REDUCTION OF CASSITERITE

## CONCENTRATE BY CHARCOAL

4. Theory : (A) Obtaining kinetic data.....	14
(B) reaction of carbon with carbon dioxide	21
(C) tin smelting slags.....	24
5. Apparatus.....	25
6. Experimental procedure.....	25
7. Sample preparation and experimental schedule.....	29
8. Results: (A) rate and extent of reaction.....	32
(B) degree of cassiterite reduction.....	43
(C) exit gas composition.....	46
9. Discussion.....	47

## CHAPTER THREE: REDUCTION OF CASSITERITE CONCENTRATE

## BY CARBON MONOXIDE

10. Theory: Obtaining kinetic data.....	62
11. Apparatus.....	65
12. Experimental procedure and schedule.....	67
13. Results.....	69
14. Discussion.....	72

## CHAPTER FOUR: CONCLUSIONS..... 80

## References..... 82

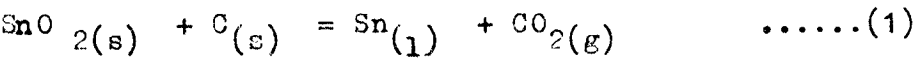
## Appendices..... 85

CHAPTER ONE: GENERAL SECTION

1. INTRODUCTION

Pyrometallurgical tin production involves the smelting of tin concentrate with anthracite coal or coke, usually in reverberatory furnaces. The smelting process is well discussed in the literature <sup>1,2</sup>.

The reduction reaction is generally represented by the chemical equation.



However, work by numerous researchers <sup>3-9</sup> on the reduction of metal oxides by carbon leads one to envisage a two-step reaction scheme comprised of:-



in which the rate of carbon oxidation by carbon dioxide determines the overall kinetics. Where stannic oxide (SnO<sub>2</sub>) is concerned, this phenomenon was confirmed by Padilla and Sohn<sup>10</sup>.

The present work deals with the reduction of Masuku cassiterite gravity concentrate by charcoal. The experiments were aimed at identifying the factors that would influence this reaction.

Needless to say, experimentation with natural concentrates poses some problems in that close control of concentrate composition may be difficult. Nevertheless, since the work was intended to assist in the planning of smelting options for the Masuku tin deposit using locally available raw materials, it was felt the project was of some importance.

The kinetic data of the experiments was to be analysed with the assumption the rate determining step was the reaction of carbon dioxide with carbon as given by equation (3).



Other experiments to be done were to involve the reduction of cassiterite concentrate by carbon monoxide in a bid to understand further the  $\text{SnO}_2$  + carbon reaction by considering reaction (2) only, of the two-step reduction process.

## 2. THE SOURCE AND ANALYSIS OF CASSITERITE CONCENTRATE

Small scattered deposits of cassiterite covering an area of about 1000 square kilometres occur in Zambia's southern province. The total tonnage of these deposits, estimated at 215 tonnes<sup>11</sup>, and the mode of occurrence do not favour large scale exploitation. Small scale mining produces at best an estimated 20 tonnes per annum of cassiterite gravity concentrate<sup>14</sup>.

According to Legg<sup>12</sup>, primary tin mineralisation in this area occurs in pegmatites of various types. Derived from such pegmatites have been the easily worked eluvial and alluvial deposits. The grade and mineralisation in all these deposits is very erratic. The cassiterite may be accompanied by tantalum, niobium, iron, manganese and arsenopyrite but even in a single pegmatite the actual composition can vary widely.

The actual source of the cassiterite concentrate used in the reduction experiments could not be ascertained but its analysis is given in Table 1. The concentrates have been so named after the locality of the supplier.

Table 1: Chemical composition of Masuku cassiterite gravity concentrate

Compound	SnO <sub>2</sub>	Fe <sub>2</sub> O <sub>3</sub>	SiO <sub>2</sub>	Al <sub>2</sub> O <sub>3</sub>	CaO	MnO <sub>2</sub>	Nb <sub>2</sub> O <sub>5</sub>	Ta <sub>2</sub> O <sub>5</sub>
Weight %	66.2	6.6	8.1	4.1	2.3	nd	nd	nd

nd = not detected

The analyses were done by XRF and wet chemical methods.

Optical microscopy revealed the cassiterite occurred as fairly free coarse grains but was occasionally attached to, or surrounded by quartz and hematite.

The size analysis of the as-received concentrate is shown in Table 2. This is given merely for the sake of completeness, in view of the remarks made concerning the nature of the deposit.

Table 2: Sieve size analysis of the as-received concentrate

ASTM mesh size	Size in mm	Weight %	Cumulative weight %
+ 4	+4.76	5.5	5.5
-4 + 6	-4.76 + 3.36	14.8	20.3
-6 + 8	-3.36 + 2.38	18.0	38.3
-8 + 10	-2.38 + 2.00	16.7	55.0
-10 + 12	-2.00 + 1.41	0.7	55.7
-12 + 16	-1.41 + 1.19	12.1	67.8
-16 + 25	-1.19 + 0.707	12.2	80.0
-25 + 35	-0.707 + 0.500	5.7	85.7
-35	-0.500	14.3	100.0

Legg<sup>13</sup> contends that, though tin losses may be high, by panning, the small scale miners produce concentrates averaging 65% SnO<sub>2</sub>. Accompanying the cited economic report<sup>11</sup> were results of mineral dressing tests done on the tin-tantalite ores. These tests showed beneficiation of cassiterite could be improved by sluicing instead of panning.

It was also shown that the concentrate obtained could be further upgraded and separation of the valuable columbite - tantalite content, achieved by a combination of tabling, magnetic separation and flotation.

As the concentrate received for the present work, fortunately had no tantalite - columbite minerals and was of a quite typical grade for tin smelting (usually 70-77% tin after extensive processing<sup>15</sup>) no attempt was made to upgrade it.

### 3. Theory

#### (A) Thermodynamics

##### (i) Carbon as a reductant

From Gibbs energy considerations, the minimum temperature at which a mixture of stannic oxide and carbon commences to react can be calculated.

Using the data in Table 3, Figure 1 was constructed from which can be seen, the minimum such temperature is 627°C assuming the reaction is of solid-solid type yielding CO<sub>2</sub> by equation (1).

Table 3: Summary of Gibbs energy data used in constructing Figures 1 and 2.

Equation	$\Delta G^\circ$ in Cal.	Temp.range(K)	Reference
$C_{(s)} + \frac{1}{2} O_{2(g)} = CO_{(g)}$	-26,700-20.95T	298 - 2500	16
$C_{(s)} + O_{2(g)} = CO_{2(g)}$	-94,200-0.2T	298 - 2000	16
$Sn_{(s)} + O_{2(g)} = SnO_{2(s)}$	138,730-48.54T	298 - 505	17
$Sn_{(l)} + O_{2(g)} = SnO_{2(s)}$	138,500-48.92T	505 - 1898	17

The carbon dioxide formed is then available to react with the surrounding carbon to form carbon monoxide according to the equation



Referring to Figure 1 again, the theoretical minimum temperature at which this is feasible is 707°C.

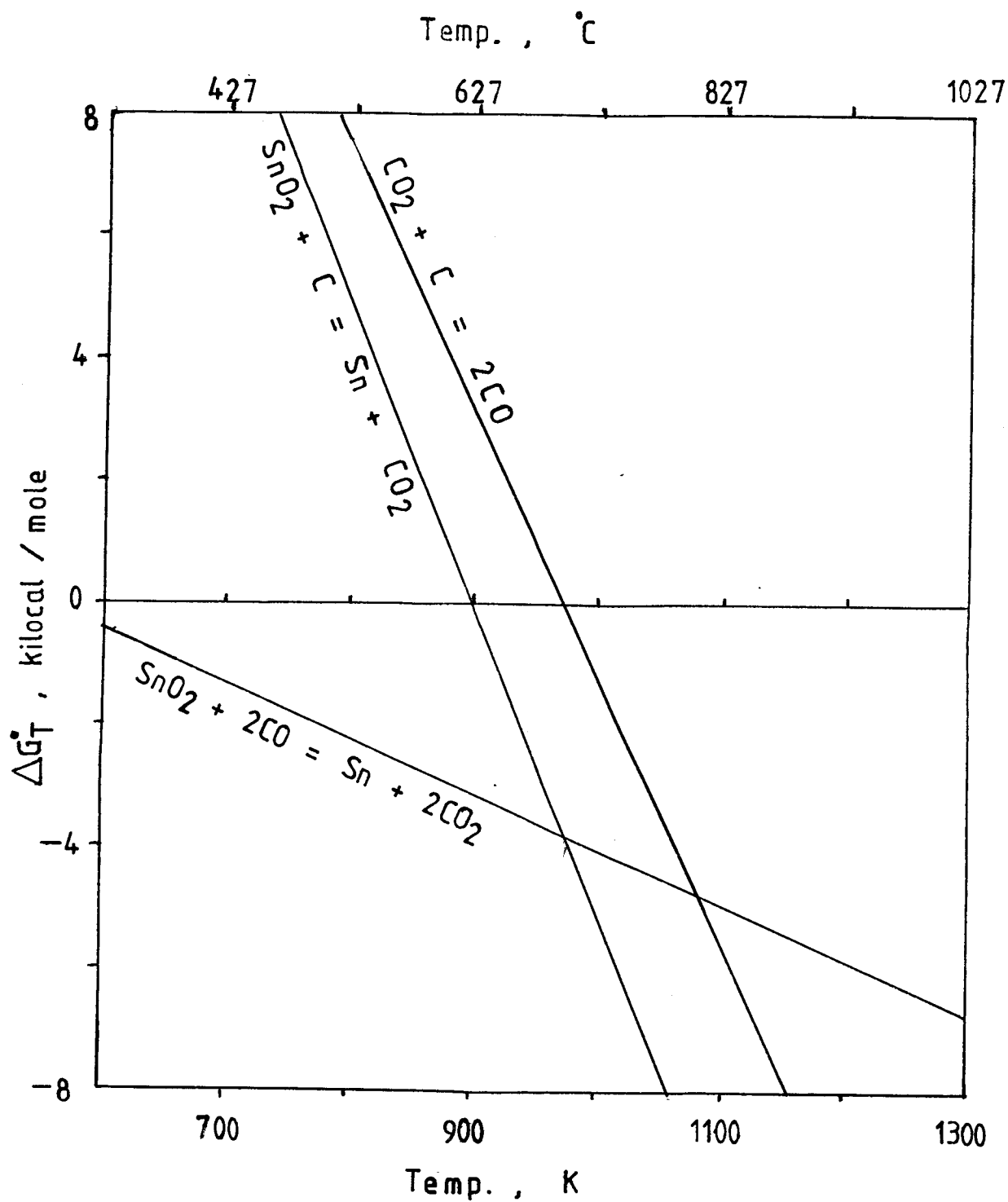


Fig.1: Graphical representation of Gibbs energy data for  $\text{SnO}_2$  reduction by carbon and CO

Hence,  $\text{SnO}_2$  reduction ought to be thermodynamically more favourable the higher the temperature.

(ii) Distribution of major impurities during tin smelting.

The normal abundant species associated with cassiterite are  $\text{Al}_2\text{O}_3$ , iron oxides and  $\text{CaO}$ . Some  $\text{Nb}_2\text{O}_5$  and  $\text{Ta}_2\text{O}_5$  and accompanying  $\text{MnO}_2$  may also be present.

Referring to Figure 2 and the Ellingham diagram in Figure 3 it can be seen that by maintaining an atmosphere just reducing for  $\text{SnO}_2$  reduction the distribution of the above named species whilst tin smelting would be as follows:-

- (a)  $\text{SiO}_2$ ,  $\text{Al}_2\text{O}_3$ ,  $\text{CaO}$ ,  $\text{MnO}_2$  and  $\text{Ta}_2\text{O}_5$  would all not be reduced and would become part of the slag structure. This shows the need of  $\text{Nb}_2\text{O}_5$  and  $\text{Ta}_2\text{O}_5$  separation, if present in the concentrate, prior to smelting.
- (b)  $\text{Fe}_2\text{O}_3$  would be reduced to  $\text{Fe}_3\text{O}_4$  which would in turn proceed to  $\text{FeO}$ . Some of this  $\text{FeO}$  may be further reduced to the metallic state. These reactions would represent a waste of the reductant and also result in contamination of the tin produced.

It is of course to be noted that the usefulness of both Figures 2 and 3 is limited due to changes that occur to the diagrams when the activities of reacting species are different from unity.

Therefore, in the absence of known activity data, for closely positioned equilibrium lines of the  $\text{Sn-Fe-C-O}$  system the remarks made above may not be quite accurate.

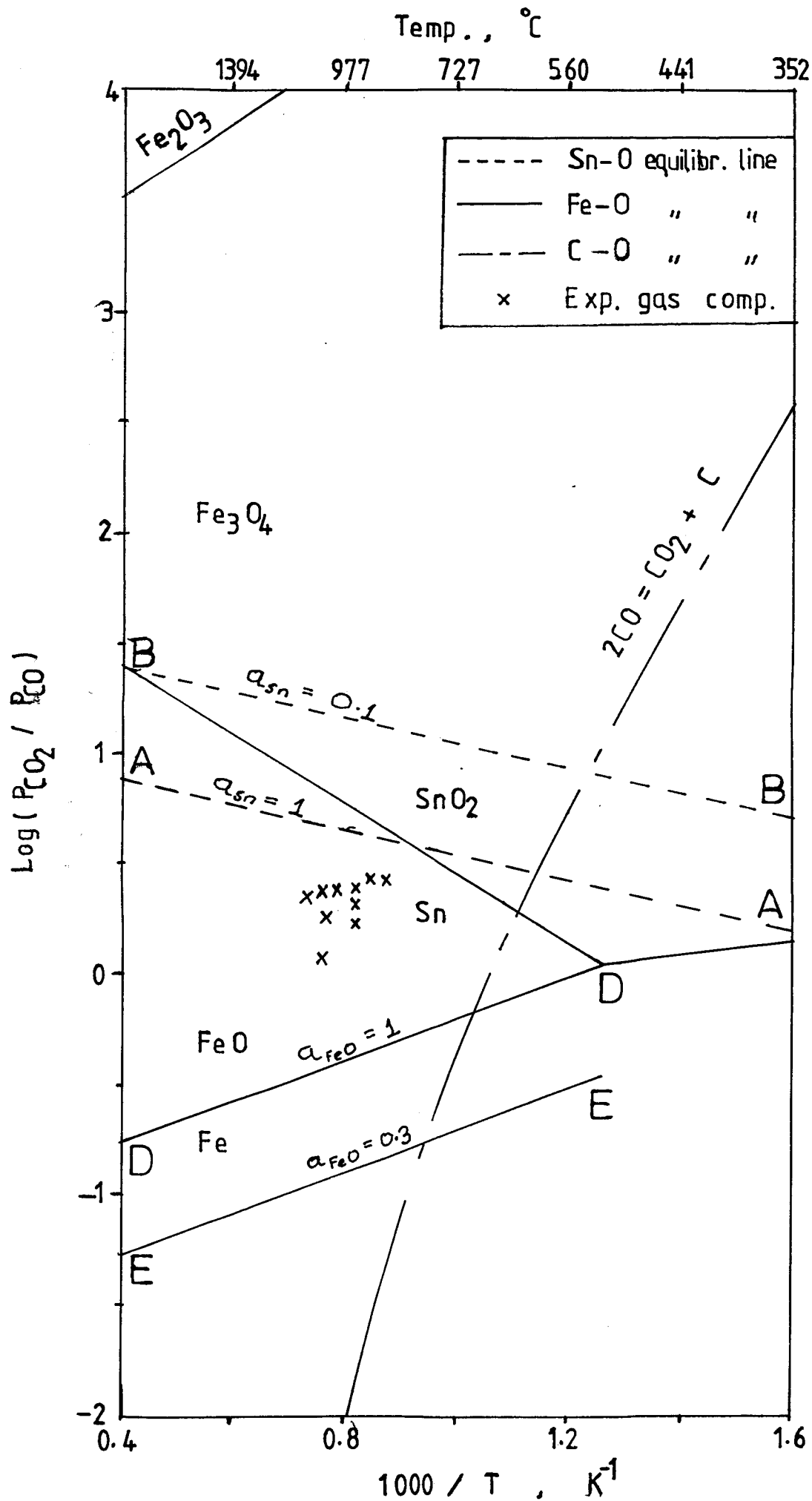


Fig. 2 : Sn-Fe-C-O System



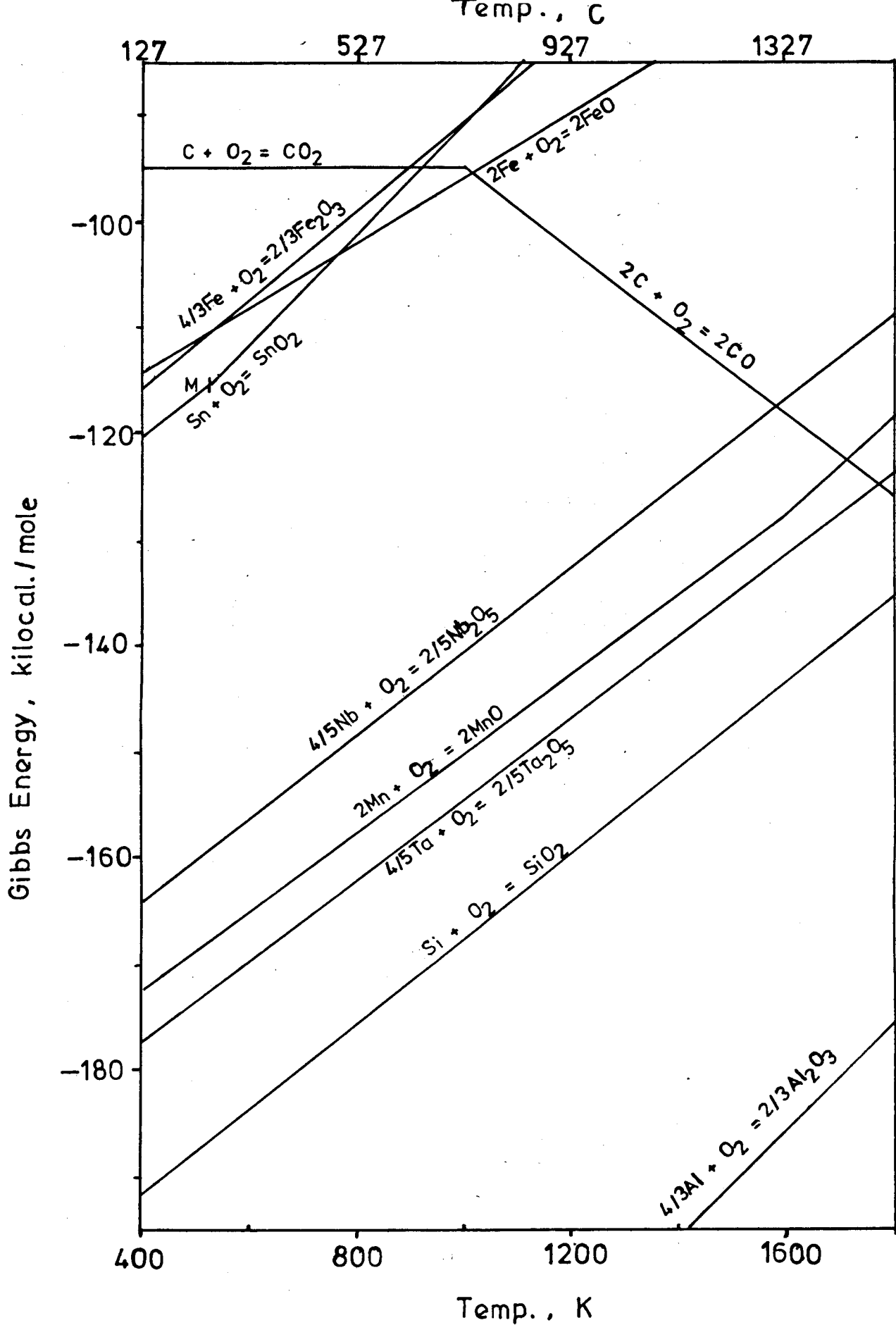


Fig. 3: Ellingham diagram for selected oxides

For instance, line B-B on Figure 2 shows the shift of the  $\text{SnO}_2(\text{s}) / \text{Sn}(\text{l})$  equilibria from A-A when the activity of tin changes from unity to 0.1. Impurities could lower the activity of tin. Similarly, when for example the activity of FeO changes from unity to 0.3, line D-D shifts to E-E. Choice of suitable slag composition could enable the decrease of FeO activity possible.

The utility of Figures 2 and 3 is further limited by their failure to take into account kinetic factors, whose effect may infact be so important as to determine whether a thermodynamic prediction occurs or not.

#### (B) Effect of temperature on kinetics

For most chemical reactions, the rate of reaction increases in a manner that conforms with Arrhenius law, which mathematically is expressed as:-

$$\ln k = \ln A - E_A/RT \dots\dots\dots(11)$$

where k is the rate constant at temperature T

A, the frequency factor

$E_A$ , the activation energy

and R, the general gas constant.

with ?

The Arrhenius rate law may be obeyed over the whole temperature range or in some restricted intervals. Major departure of data from the law is usually the sign of a complex reaction mechanism or changes in the dominant mechanism over the temperature range studied<sup>19</sup>.

Equation (11) shows that at a particular temperature, the rate of reaction is obtained by a knowledge of two independent terms, namely

- (a) the frequency factor,  $A$ , and
- (b) the energy of activation,  $E_A$ .

One view, the collision theory, suggests that " $A$ " is equal to the frequency of collisions between reacting molecules. With some modifications this approach has been used to predict values of the frequency factor with some measure of success <sup>20</sup>.

Another theoretical approach which has given good agreement with actual determined values of the frequency factor is the transition state theory. In this theory, " $A$ " is expressed as a product of parameters among which are partition functions. The partition function of a molecule per unit volume is a measure of the probability of occurrence of that molecule in the specified volume.

From both theories it can be seen that the frequency factor depends on the particular reaction in question and the experimental assembly used to effect the reaction.

The activation energy is on the other hand readily determined <sup>18</sup>, either graphically or by calculation from a knowledge of rate constant data at two or preferably more values of temperature in the range where the Arrhenius law is obeyed. Strictly speaking the activation energy can only be computed for a well defined reaction step. For more complex phenomena it is still used, though only as a rough indication of the minimum average kinetic energy that molecules require to initiate a reaction and to show the possible type of rate determining step.

Activation energies for processes controlled by physical phenomena are generally less than about 20 kilocalories per mole while those for processes controlled by chemical reactions are of the order 10-100 kilocalories per mole.

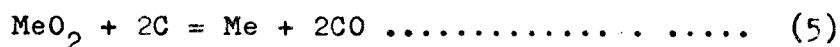
CHAPTER TWO:        REDUCTION OF CASSITERITE CONCENTRATE BY  
CHARCOAL

4.    Theory

(A)   Obtaining kinetic data

Many methods exist for measuring the rate at which a reaction proceeds <sup>20</sup>. The suitability of any particular method depends on the nature of the reaction being investigated.

For a solid-solid type of reaction yielding a condensed phase and some gaseous product, the weight loss method provides a convenient measure of the extent to which a reaction has occurred. If the reduction of a metal oxide ( $\text{MeO}_2$ ) by carbon is represented by:



and given ( $\text{MeO}_2$ ) and (Me) are not volatile in the temperature range of interest, the weight loss in the reaction mixture would correspond to the weight of  $\text{CO}_2$  and CO evolved. The oxygen component of the evolved  $\text{CO}_2$  and CO would be that derived from  $\text{MeO}_2$  as it is reduced to (Me). A knowledge of the rate of  $\text{CO}_2$  and CO evolution would therefore facilitate a study of the rate of (Me) formation from ( $\text{MeO}_2$ ).

Equations (4) and (5) do not indicate the mechanism by which the reduction of metal oxide ( $\text{MeO}_2$ ) occurs, but for the purposes of thermodynamic analysis which only depends on the initial and final states of the system under consi-

deration, the two equations may be used to obtain the amount of tin produced and that of carbon reacted.

Considering an  $\text{SnO}_2$  and carbon reaction mixture, both  $\text{SnO}_2$  and Sn are not volatile and in particular, for Sn the vapour pressure is only  $10^{-4}$  mm Hg at  $1000^\circ\text{C}$  <sup>16</sup>.

It is therefore possible to utilise the weight loss method to determine the rate of  $\text{SnO}_2$  reduction.

Srinivasan and Lahiri <sup>4</sup> followed the progress of haematite ore reaction with graphite by means of sample weight change and  $\text{CO}/\text{CO}_2$  gas analysis. The sample weight loss was monitored continuously by a balance to which the haematite/graphite pellet was attached. Gas analysis was done gravimetrically. The weight of  $\text{CO}_2$  gas produced in a particular time interval was measured as the increase in weight of absorption tubes filled with soda asbestos and magnesium perchlorate. At any instant, liberated CO was evaluated as the difference between sample weight loss and the corresponding  $\text{CO}_2$  absorption data.

Their determined values of  $\text{CO}_2/\text{CO}$  ratio at  $1022^\circ\text{C}$  are shown in Figure 4 which has been reproduced from their paper.

Using constant pellet diameter and nitrogen flow, the effect of carbon/haematite relative amounts on the gas composition was also studied. The results are included on the same diagram. Coupled with X-ray diffraction studies of reduced pellets, the variation of  $\text{CO}_2/\text{CO}$  ratio was explained in terms of the stepwise reduction of  $\text{Fe}_2\text{O}_3$  through  $\text{Fe}_3\text{O}_4$  and  $\text{FeO}$ , giving finally Fe metal.

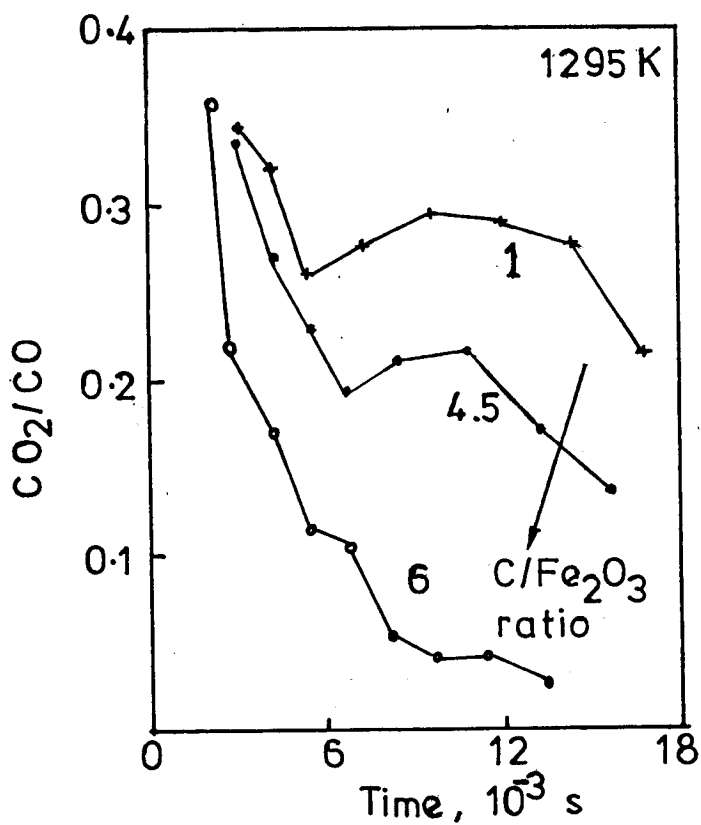


Fig. 4: Exit gas  $\text{CO}_2/\text{CO}$  ratio as a function of time.

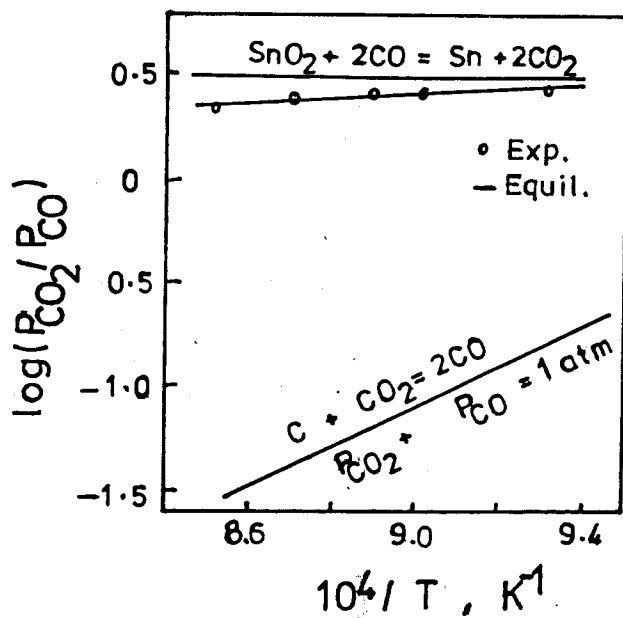


Fig. 6:  $\text{CO}_2/\text{CO}$  ratios for  $\text{SnO}_2/\text{C} = 1/2$ .

The lower  $\text{CO}_2/\text{CO}$  ratios at higher relative amounts of carbon in the pellet were attributed to the higher carbon gasification rate to form CO.

Whilst studying the factors affecting the reduction of Zinc oxide by carbon, Hopkins and Adlington <sup>3</sup> also measured  $\text{CO}/\text{CO}_2$  ratios during the course of reduction. Using intimate mixtures of pure ZnO (99.9%) and degassed carbon black in silica retorts the  $\text{CO}/\text{CO}_2$  profile was established. Nitrogen was used to transport the produced gases. In given time intervals, they too, measured  $\text{CO}_2$  evolved by observing the increase in weight of soda asbestos absorbers. The remaining off-gas containing CO was mixed with pure dry oxygen and passed over a platinised asbestos catalyser kept at  $700^\circ\text{C}$  before determination of CO as  $\text{CO}_2$  in a second soda asbestos absorber.

Figure 5 summarises the results for this part of their research. The dotted lines show the temperature at which the charge reached the operating temperature. At low temperatures, the limitation of weighing minute amounts of gas was pointed out, while at high temperatures it was the difficulty of ensuring complete absorption of the oxidised CO in the absorber. It was found apparent nevertheless that the retort atmosphere quickly reached a steady value of  $\text{CO}/\text{CO}_2$  ratio when the temperature became constant.

An application of the Gibbs phase rule to the reduction of metal oxide  $\text{MeO}_2$  by carbon can allow prediction of whether the  $\text{CO}/\text{CO}_2$  ratio would vary or not in the course of the reaction.

Charge composition ,  $\text{ZnO} / \text{C} = 2$

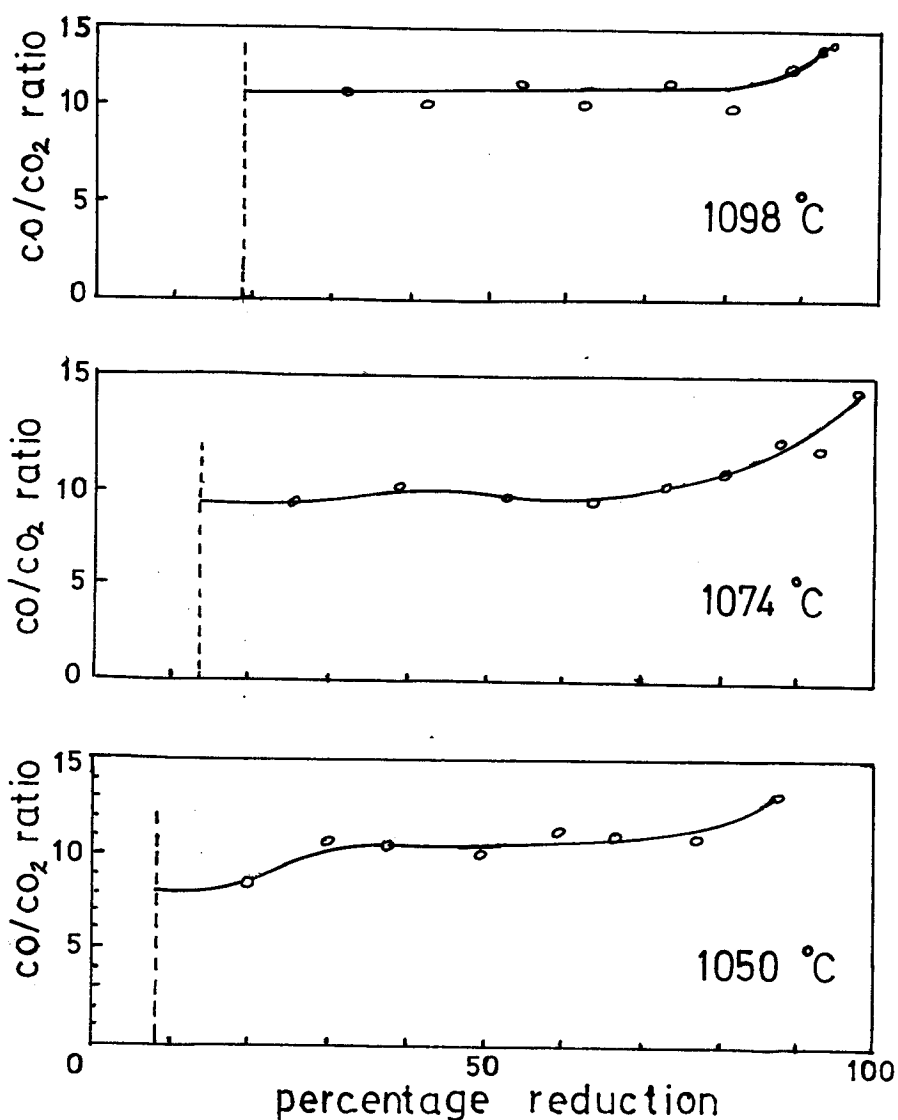


Fig. 5 : The variation of  $\text{CO}/\text{CO}_2$  ratio during the reduction of zinc oxide by carbon black at various temperatures.



For example, for the reduction of pure  $\text{MeO}_2$  to Me in a single step by carbon conducted at a constant pressure and temperature the  $\text{CO}/\text{CO}_2$  ratio can be shown to be one that would be invariant. For common metallurgical uses where temperature and pressure are the only environmental factors that can be independently varied, the phase rule can be written as <sup>22</sup>:

$$F = C - P + 2$$

where F denotes the number of degrees of freedom of the system and C is the number of components present in P phases.

With the restriction of isothermal and isobaric conditions the phase rule takes the form

$$F = C - P \dots\dots\dots (6)$$

For the case being considered,

C = 4; namely four out of  $\text{MeO}_2$ , Me, C, CO,  $\text{CO}_2$ .

P = 4;  $\text{MeO}_2$ , Me, C and the gas phase.

Substitution of these values into (6) shows the system to be invariant.

In their paper<sup>10</sup> on the reduction of stannic oxide by carbon Padilla and Sohn concluded that  $\text{SnO}_2$  was reduced directly to tin. As is to be expected therefore, they reported only a single value of  $\text{CO}/\text{CO}_2$  ratio at any particular temperature as shown in Figure 6 which is reproduced from their paper.

They measured in a nitrogen flow the gas composition arising from the reaction by gas chromatography. By measuring the  $\text{CO}/\text{CO}_2$  ratio they wanted to gain an insight into the rate of the Boudouard reaction as compared to that of stannic oxide reduction by carbon monoxide.

In the present work,  $\text{CO}_2$  and CO gas analyses and sample weight loss data were used conjointly to determine the amount of metal formed from stoichiometry considerations of equations (4) and (5).

(B) Reaction of carbon with carbon dioxide

The gasification of carbon by  $\text{CO}_2$  can be represented by:



Rao and Jalan <sup>23</sup> have presented a simplified picture of the successive steps involved in this reaction. These are listed below.

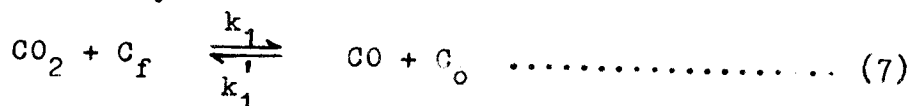
- (a) External transport of  $\text{CO}_2$  to the surface of carbon
- (b) Pore diffusion of  $\text{CO}_2$  into the carbon
- (c) Chemisorption of  $\text{CO}_2$  on the carbon surface
- (d) Surface reaction
- (e) CO desorption from the reaction surface
- (f) Pore diffusion of CO outward
- (g) External transport of CO from the carbon surface.

Clearly, step (a) is of no concern for present purposes.

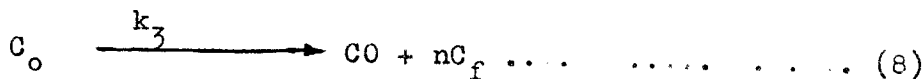
It was necessary for the work of Rao and Jalan since they considered the oxidation of carbon in a  $\text{CO}_2$  stream.

Thus, only steps (b) and (f) are left as transport processes while the others are chemical in nature. It has been reported <sup>24</sup> that Duval demonstrated pore diffusion could not be the rate limiting step. In one series of his experiments, gasification of carbon filaments at different temperatures followed by determination of roughness factors of the filaments by the BET method revealed the roughness factors remained invariant even when the rates of carbon burn-off were different.

Attention may thus be focused on the surface reaction mechanism. According to Ergun <sup>25</sup>, the gasification sequence consists of initial CO<sub>2</sub> - carbon interaction represented by:



followed by transfer of carbon to the gas phase as shown by:



where C<sub>o</sub> is an active site occupied by oxygen,  
C<sub>f</sub> is a site free of oxygen,

k<sub>1</sub>, k<sub>1</sub>', k<sub>3</sub> are rate constants, which are  
functions of temperature only,

and n is an integer equal to 0, 1, or 2.

Statistically 0 ≤ n ≤ 2. For n > 1, the number of reaction sites increases with gasification. When n = 1 the number of reaction centres remains constant while for n < 1 the carbon gets less active with burn-off.

Reaction (7) is said<sup>6</sup> to be extremely fast so that (8) forms the rate controlling step.

The instantaneous rate of gasification of carbon at a constant temperature surrounded by a gas of uniform composition may be expressed as <sup>23, 25, 26</sup>:

$$-\frac{dW^c}{dt} = k_3 W^c (C_o) \dots\dots\dots (9)$$

$$\text{or } -\frac{dW^c}{W^c} = k_3 (C_o) dt$$

where (C<sub>o</sub>) is the concentration of oxygen occupied sites  
per gram of carbon.

and W<sup>c</sup> is the instantaneous weight of carbon

Integration of equation (9) requires a knowledge of the variation of  $(C_o)$  with reaction time. However, during the early stages of the reaction  $(C_o)$  can be considered constant.

$$\therefore \quad \frac{-dw^c}{w^c} = R_c dt$$

where  $R_c$  is a rate constant that incorporates the condition of active sites on the carbon surface.

Integrating between  $w^c = w_o^c$  at  $t = 0$

and  $w^c = w_t^c$  at  $t = t$

$$\text{gives} \quad -\ln \frac{w_t^c}{w_o^c} = R_c t \dots\dots\dots(10)$$

In their paper on the rate of carbon oxidation in a carbon dioxide stream, Rao and Jalan<sup>23</sup> found the above equation to adequately fit the experimental data up to the stage of 25% carbon burn-off. Work by Padilla and Sohn<sup>10</sup> demonstrated that the rate of carbon oxidation by carbon dioxide determines the overall kinetics of stannic oxide reduction by carbon. Therefore, it was found fitting to attempt the analysis of kinetic data obtained in the present work with the aid of equation (10).

(C) Tin smelting slags

Different opinions have been expressed as to how the best slag for tin smelting can be obtained.

Some authors<sup>27</sup> have reported that slag calculations can be best made based on a slag pH value of 1.25 to 1.5 and a molar ratio of FeO to CaO in the slag equal to unity. Others<sup>28</sup> have used the expression:

$$\frac{\% \text{CaO} + \% \text{FeO}}{\% \text{SiO}_2 + \% \text{Al}_2\text{O}_3}$$

as a measure of the basicity of tin free slags with typical values being in the range 0.7 to 2.0. Slags chosen on the basis of the low melting point (1093-1100°C) region of Levin and McMurdie's<sup>21</sup> CaO-FeO-SiO<sub>2</sub> system on the other hand, have a composition approximating 14%CaO, 50%FeO and 36%SiO<sub>2</sub>.

Consideration of the above views led to the addition of small amounts of lime to some of the cassiterite samples to be reduced.

### 5. Apparatus

The common experimental set-up for thermogravimetric analysis shown in Figure 7 was used. An alumina sample crucible (4) was enclosed in a platinum wire basket and suspended from a balance (1) by means of a wire of the same material. The sample hung in the centre of a silica reactor (3) well clear of its sides.

Heating of the reactor was achieved by means of a vertical tube furnace rated up to  $1200^{\circ}\text{C}$ , which held the reactor centrally. On the upper part of the silica tube, external to the furnace was a side tube through which a low flow of nitrogen gas was introduced to maintain an inert atmosphere in the reactor. The exit gases proceeded to an orsat gas analyser (6). Depending on the position of the stop-cock on the analyser, the gases could enter the measuring burette or be vented into the air.

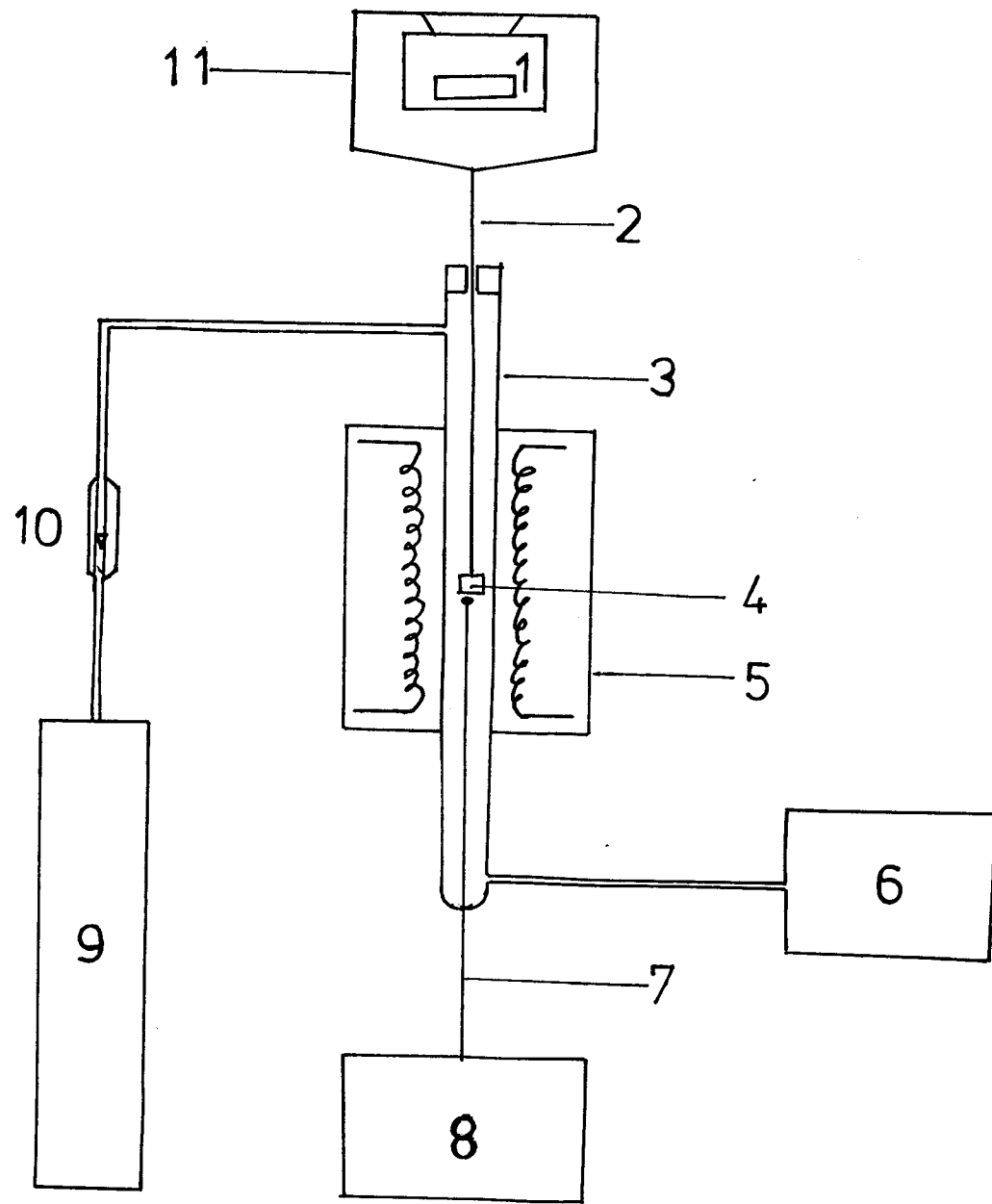
The temperature near the sample was measured by a thermocouple (7) introduced through the bottom of the reactor with its hot junction positioned just beneath the sample crucible. The other end of the thermocouple was connected to a potentiometer (8) which gave the temperature directly in degrees centigrade.

The orsat gas analyser was the usual three bulb type <sup>29</sup> in which only two bulbs were filled. One bulb had 30% W/V KOH for  $\text{CO}_2$  absorption and the other 10% W/V acid cuprous chloride solution for CO absorption. Oxygen gas analysis was unnecessary.

### 6. Experimental procedure

The ideal experimental set-up for work undertaken in this study would have been that giving a continuous record of sample weight loss and product gas analysis at a set temperature in a totally inert atmosphere.

Fig.7: Thermogravimetric Apparatus



Balance

Platinum wire

Silica reactor ( I.D. 2.65 cm, l 95 cm )

Crucible ( O.D. 1.17 cm, I. Vol. 0.64 cm<sup>3</sup> )

Tube furnace ( l 95 cm )

10 Rotameter

Orsat gas analyser

11 Frame for load transmission

Thermocouple

Potentiometer

Nitrogen gas cylinder



With the apparatus available, an attempt to observe continuously the sample weight loss meant accepting some gas leakage from the silica reactor and probable air ingress. This was as a result of the channel in the rubber stopper at the top of the reactor through which the platinum wire had to transmit sample loads to the balance.

In order to achieve some measure of accuracy each experiment was done twice. The first time, weight loss data was obtained at fairly close time intervals. At a specified time in the course of the reaction, gas leakage was stopped by squeezing some refractory wool around the platinum wire at the top of the reactor. Exit gas was then directed into the gas analyser burette and locked there. The wool was then removed and weight loss measurements continued. Actual manipulation of the Orsat to determine gas composition was done later when free from the task of recording sample weights.

In a repeat of each experiment, the attainment of a totally <sup>desired</sup> inert atmosphere was aimed at. An unholed rubber stopper supported the sample crucible by wedging the platinum wire against the side of the silica reactor. Consequently the sample crucible was not attached to the balance. At selected time periods the sample crucible was pulled to the top of the reactor, allowed to cool, removed then weighed. Once per every time interval the sample was within the furnace, exit gas was drawn into the Orsat burette. This was later analysed while the sample cooled. Only a single determination of the gas composition could be done in each time interval the sample was within the furnace since CO absorption took a very long time.

At the conclusion of an experiment, the physical state of the reaction product was noted. The product was then left under concentrated hydrochloric acid attack for 48 hours before its tin content was determined by iodimetric titration <sup>30, 31</sup>.

Tin in unreacted cassiterite was not included in this determination due to the resistance of the latter to attack by concentrated hydrochloric acid <sup>32</sup>.

In isothermal experiments, the furnace temperature regulator was used in conjunction with the reactor thermocouple to establish the required temperature. The sample was then very quickly brought into position in the furnace. Preliminary experiments showed it took two minutes for the sample temperature to reach an isothermal temperature of 1000°C.

In experiments to investigate sample behaviour whilst being heated, the sample was introduced into a cold furnace. The furnace was then switched on and the current supply, of up to 8 amperes, to the heating coils controlled to achieve a definite heating profile.

Experiments to investigate the effect of sample porosity were conducted by ensuring different weights of reactant occupied the same crucible volume. That is, bulk density was used as a measure of porosity.

# 7. Sample preparation and experimental schedule

Preliminary experiments showed the cassiterite had no volatile matter. It was prepared into various size fractions, dried, and stored in a desiccator. A portion from each size fraction was removed and analysed for tin. Table 4 shows the tin content of the size ranges used. Decomposition of cassiterite prior to iodimetric tin analysis was achieved by fusion with a mixture of sodium carbonate and borax<sup>33</sup>.

Table 4: Tin content of prepared size fractions

Size range (microns)	-63	-90 + 63	-180 + 150	-355 + 300
Sn Content %	66.9	68.2	67.5	65.8

Charcoal was devolatilized at 925°C for 7 hours in a nitrogen atmosphere, screened into required size ranges and stored in an oven maintained at about 105°C. The charcoal so prepared analysed:-

Ash	1.57 %
moisture	0.0 %
volatile matter	0.0 %
fixed carbon	98.43 % (by difference)

Lime used was of general purpose grade. Its total chloride and total sulphur content was low however, 0.002% and 0.02% respectively while particle size analysis showed the lime was -53 microns. Before use, it was heated to 800°C and cooled. Final cooling and storage was in a desiccator.

A sizeable amount of the reactants was hand mixed to give the required composition. Unless when the effect of porosity was to be studied, samples drawn from such a mixture and charged into the alumina crucible weighed about 0.9 gram.

The experiments carried out, all under a low flow of nitrogen gas, are listed in Table 5.

Table 5: Experimental schedule

Expt. No.	Heating rate (ampere)	SnO <sub>2</sub> /C (ratio)	Charcoal size (microns)	Concentrate size (microns)
A1	8	1:1	-53	-63
A2	4	1:1	-53	-63

Expt No.	Temperature (°C)	SnO <sub>2</sub> /C (ratio)	charcoal size (microns)	concentrate size (microns)
B1	950	1:1	-53	-63
B2	1050	1:1	-53	-63
B3	950	1:1.5	-53	-63
B4	950	1:2	-53	-63
B5	1050	1:2	-53	-63
B6	950	1:4	-53	-63
B7	1050	1:4	-53	-63
C1=B1	950	1:1	-53	-63
C2	950	1:1	-106 + 75	-63
C3	950	1:1	-150 + 125	-63

Expt No.	Temperature (°C)	SnO <sub>2</sub> /C (ratio)	charcoal size (microns)	concentrate size (microns)
D1	950	1:1	-53	-90 + 63
D2	1050	1:1	-53	-90 + 63
D3	950	1:1	-53	-180 + 150
D4	1050	1:1	-53	-180 + 150
D5	1050	1:1	-53	-355 + 300
E1	850	1:1	-106 + 75	-90 + 63
E2	900	1:1	-106 + 75	-90 + 63
E3	950	1:1	-106 + 75	-90 + 63
E4	1000	1:1	-106 + 75	-90 + 63
E5	1050	1:1	-106 + 75	-90 + 63
E6	1100	1:1	-106 + 75	-90 + 63

Expt. No.	Temp. (°C)	SnO <sub>2</sub> /C (ratio)	Bulk density (g/cm <sup>3</sup> )	charcoal size (microns)	concentrate size (microns)
F1 = E5	1050	1:1	1.5	-106 + 75	-90 + 63
F2	1050	1:1	1.7	-106 + 75	-90 + 63
F3	1050	1:1	1.9	-106 + 75	-90 + 63

Expt. No.	Temp. (°C)	SnO <sub>2</sub> /C ratio	CaO content (%)	Charcoal size (microns)	concentrate size (microns)
G1	950	1:1	2.5	-106 + 75	-90 + 63
G2	1050	1:1	2.5	-106 + 75	-90 + 63
G3	1050	1:1	5.0	-106 + 75	-90 + 63

## 8. Results

### (A) Rate and extent of reaction

Most results are presented as isothermal plots of relative cumulative weight loss,  $\Delta W_t/W_0$  against time; where:-

$\Delta W_t$  = sample weight loss up to time (t).

and  $W_0$  = initial weight of the sample.

The extent of reaction as sample temperature was raised is shown in Figure 8 as a  $\Delta W_T/W_0$  versus temperature plot,  $\Delta W_T$  being the cumulative weight loss up to the temperature (T).

Data on which the plots of figures 8 to 16 were based is tabulated in the Appendices 1 to 7. A summary of the results as deduced from the graphs follows.

#### (i) Extent of reaction as sample temperature was raised

The reduction of Masuku cassiterite concentrate with charcoal commenced in the neighbourhood of  $850^\circ\text{C}$  while the rate of reduction was found to increase rapidly in the temperature interval of 1000 to  $1050^\circ\text{C}$ . Figure 8 further shows that if allowance was made for the sample to come to equilibrium at each temperature, the figures quoted above would have been somewhat lower.

#### (ii) Influence of relative amounts of reactants

Experiments were conducted with constant particle size of reactants. The molar ratio of  $\text{SnO}_2$  to carbon was varied from 1:1 to 1:4. It is clear from figure 9 that at the same temperature, as the reductant content increased the rate of reduction rose. In conjunction with data from figure 10, the combined effect of  $\text{SnO}_2$  to carbon ratio

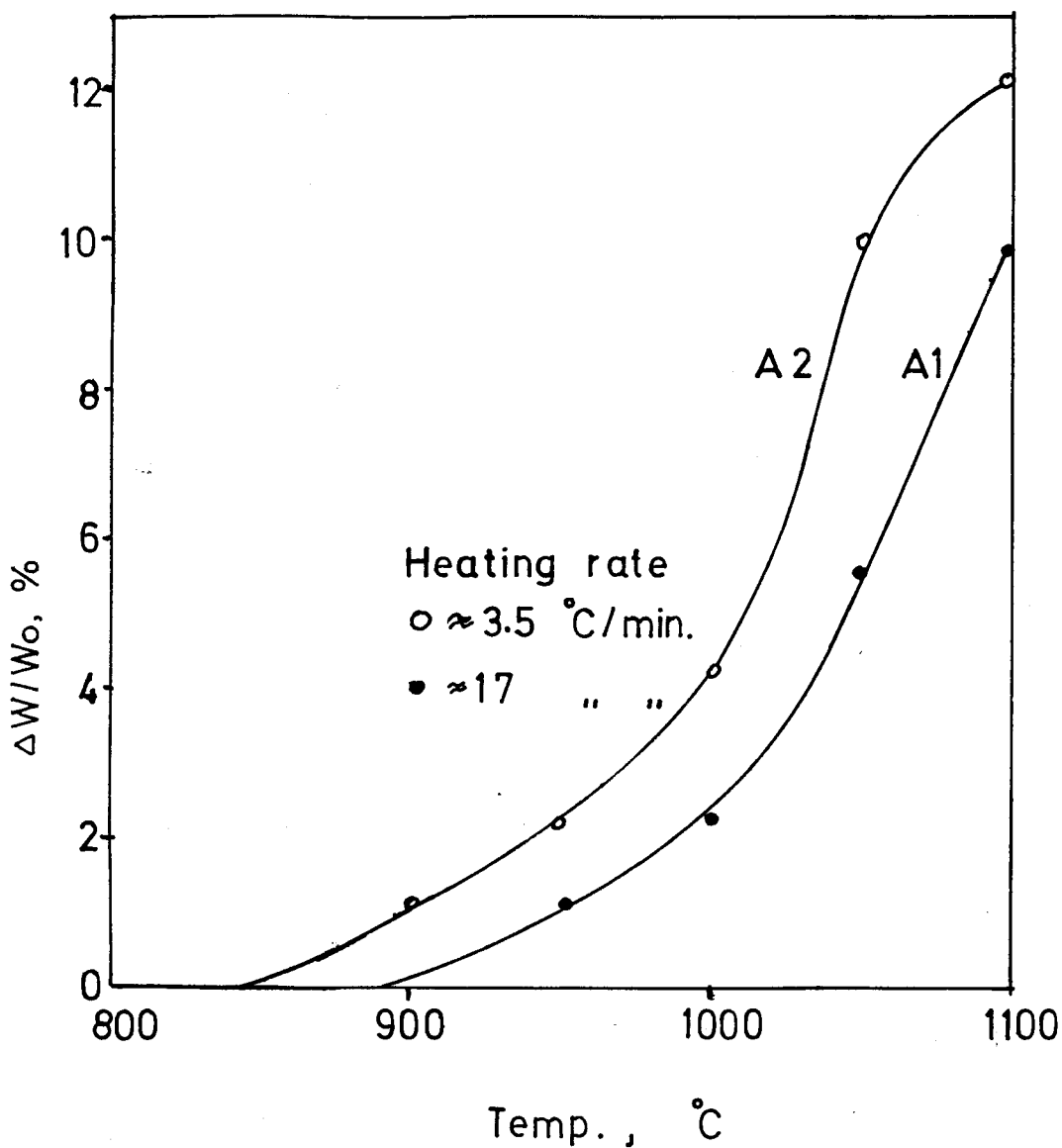
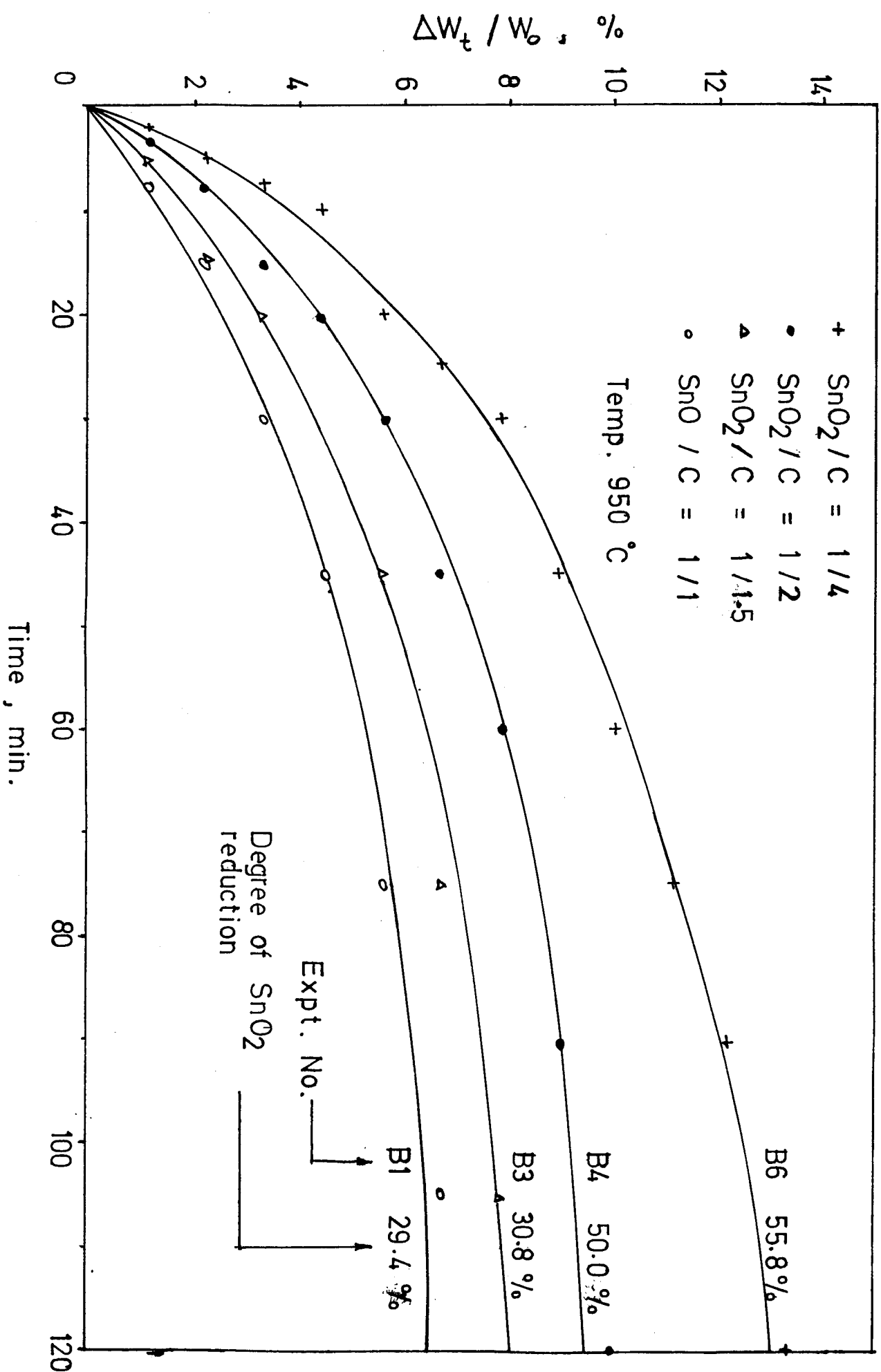


Fig. 8: Extent of reaction as sample temperature was raised

- +  $\text{SnO}_2 / \text{C} = 1 / 4$
- $\text{SnO}_2 / \text{C} = 1 / 2$
- ▲  $\text{SnO}_2 / \text{C} = 1 / 1.5$
- $\text{SnO} / \text{C} = 1 / 1$

Temp. 950 °C





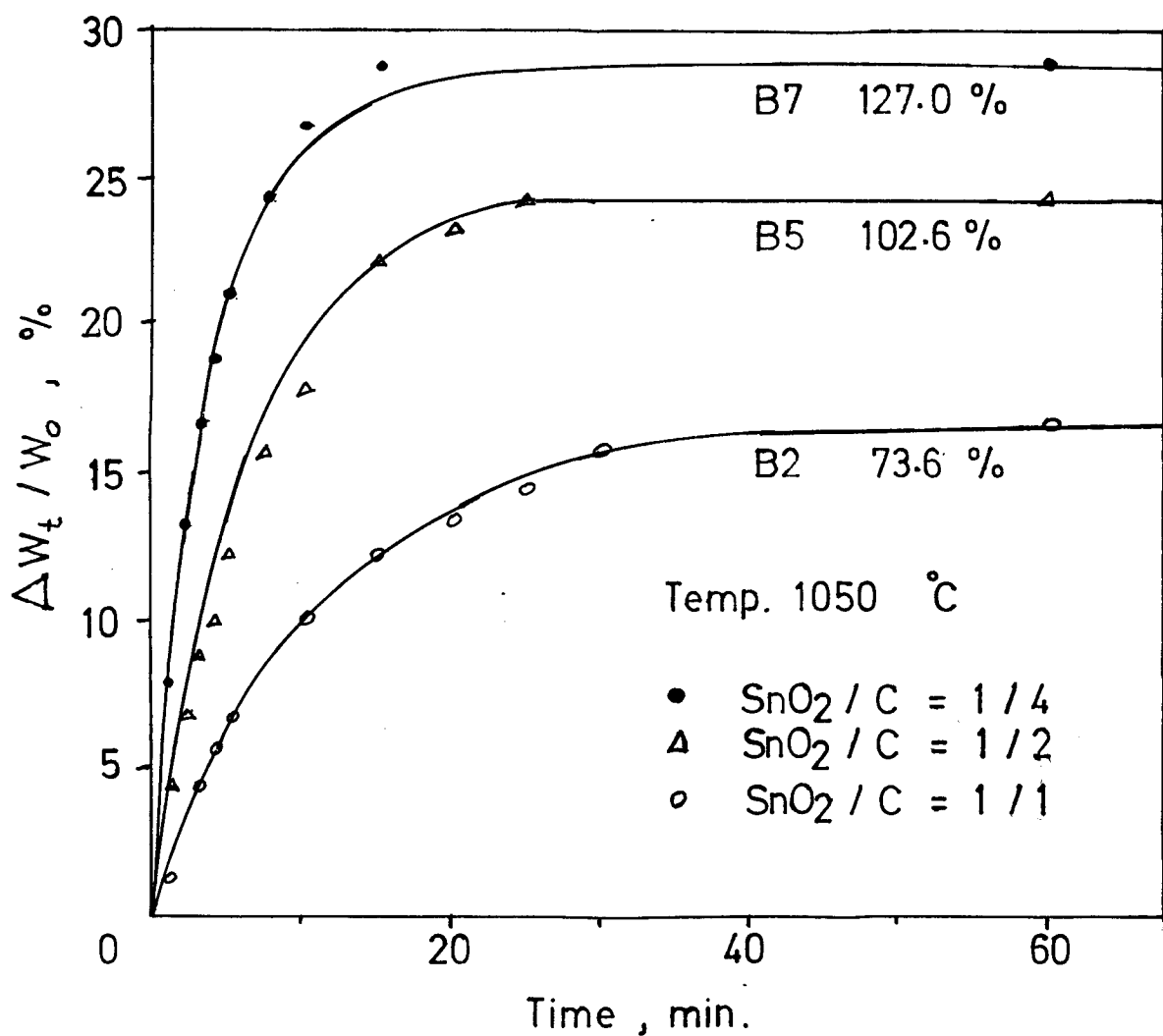


Fig.10 : Dependence of rate of reaction on the relative amount of reactants

and temperature is assessed below.

Table 6: Effect of temperature and relative reactant amounts on extent of reaction.

SnO <sub>2</sub> /C (ratio)	Time for $\frac{2}{3}$ reaction completion (min.)	
	at 950°C	at 1050°C
1:4	40	4
1:2	37	7
1:1	42	13

Table 6 shows that the rate of reduction increased markedly under the combined influence of high temperature and high reductant ratio in the reaction mixture.

(iii) Effect of charcoal particle size

Figure 11 revealed that, at a constant temperature, the reaction rate was independent of the reductant particle size within the size range investigated, of up to 150 microns. The molar ratio of the reactants and the concentrate particle size were maintained constant.

(iv) Effect of concentrate particle size (Figure 12)

Using a constant SnO<sub>2</sub>: carbon ratio of unity and the same charcoal particle size, the results of this set of experiments demonstrated that, at the same temperature, high reaction rates were favoured by fine sized cassiterite concentrate particles.

Table 7, compiled with the further aid of figure 13 showed that the additional effect of temperature increased the rate of reduction similarly in the two size ranges.

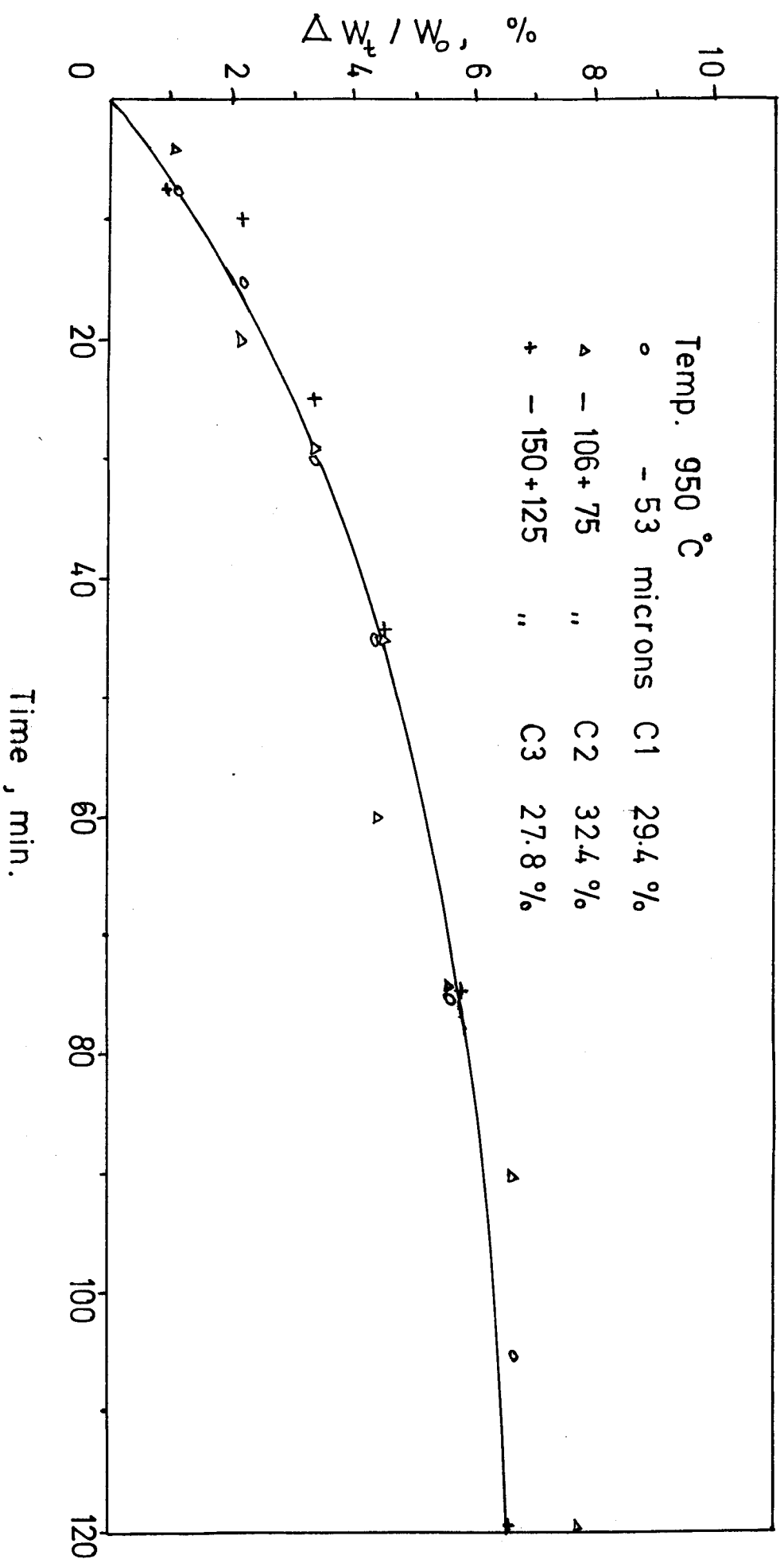
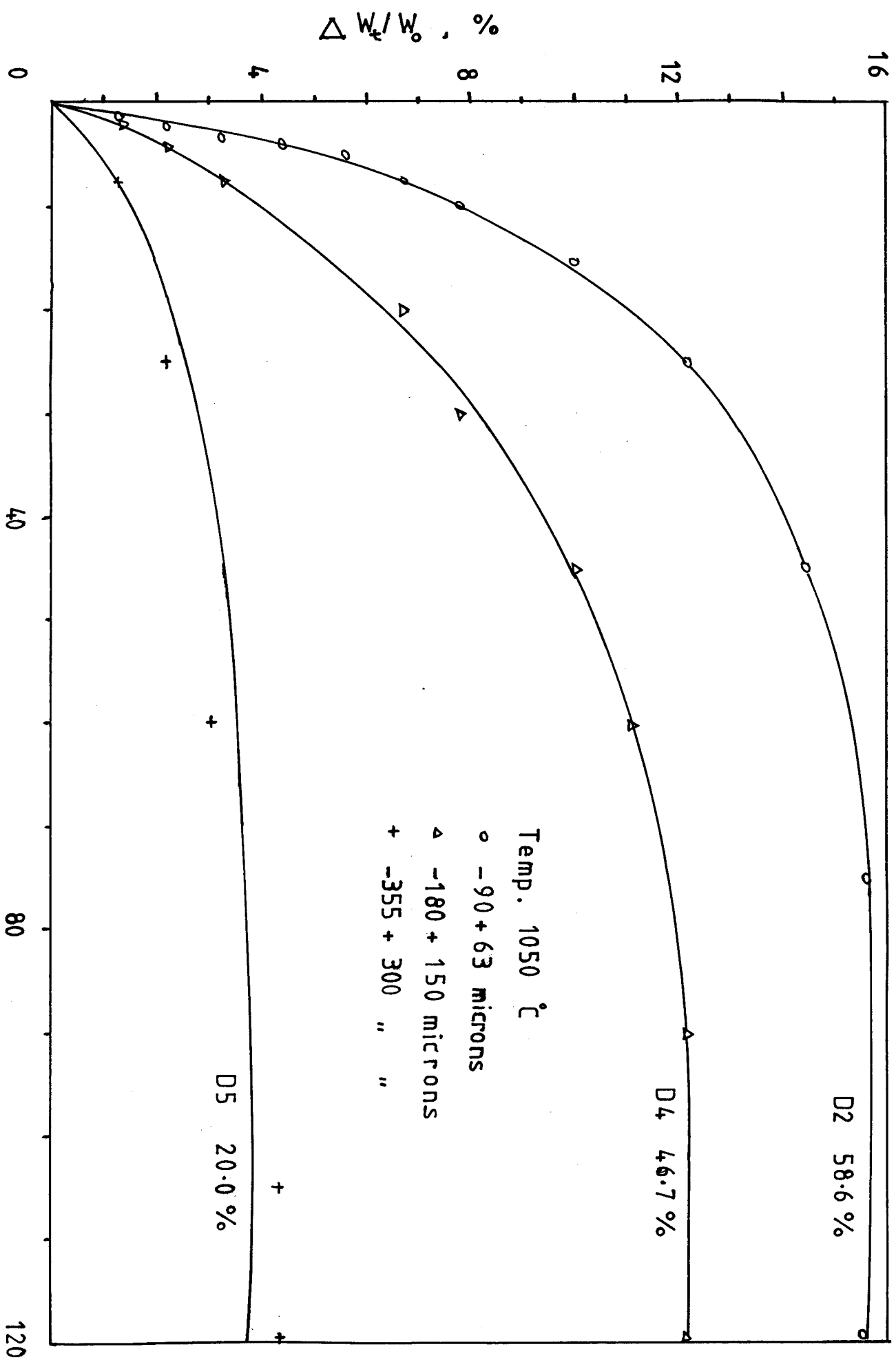


Fig.11: Effect of charcoal particle size on reaction rate



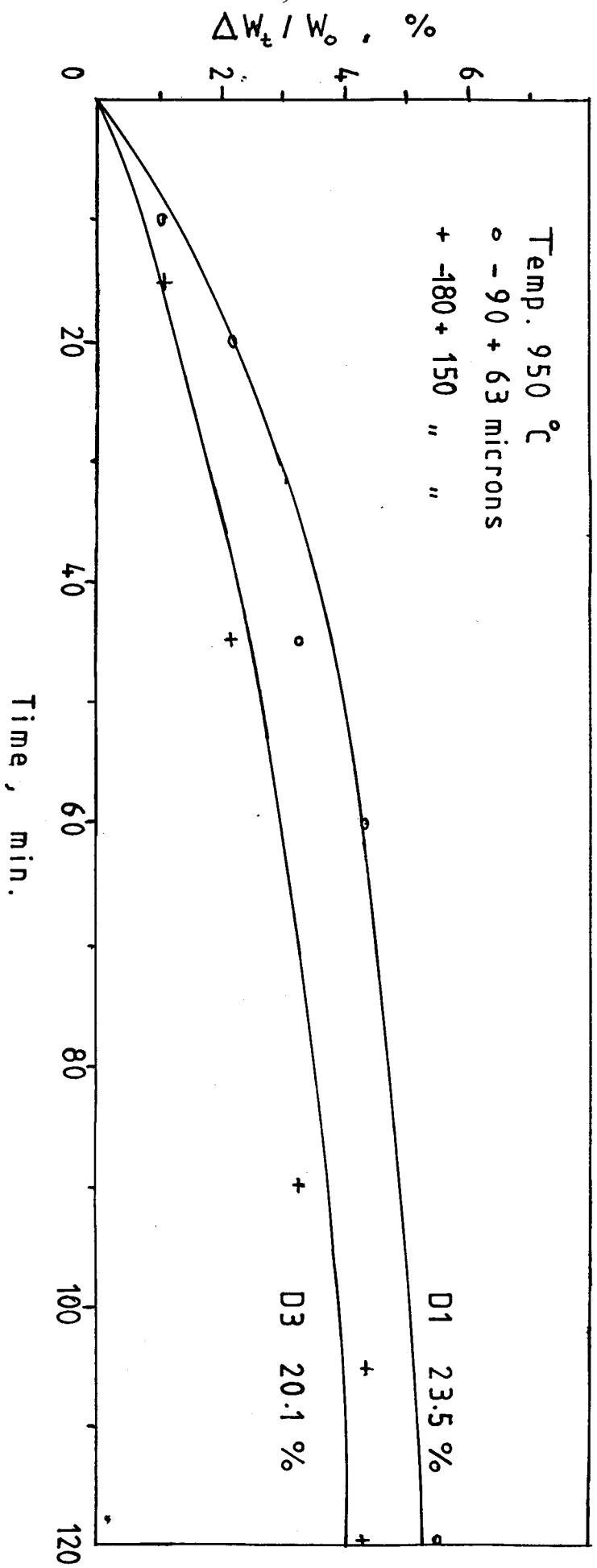


Fig. 13: Effect of concentrate particle size on reaction rate

Table 7: Combined effect of concentrate particle size and temperature.

SnO <sub>2</sub> Particle size (microns)	Time for $\frac{3}{4}$ reaction completion (minutes)	
	at 950°C	at 1050°C
-90 + 63	42	17
-180 + 150	54	25
-355 + 300	-	33

32?

(v) Influence of temperature

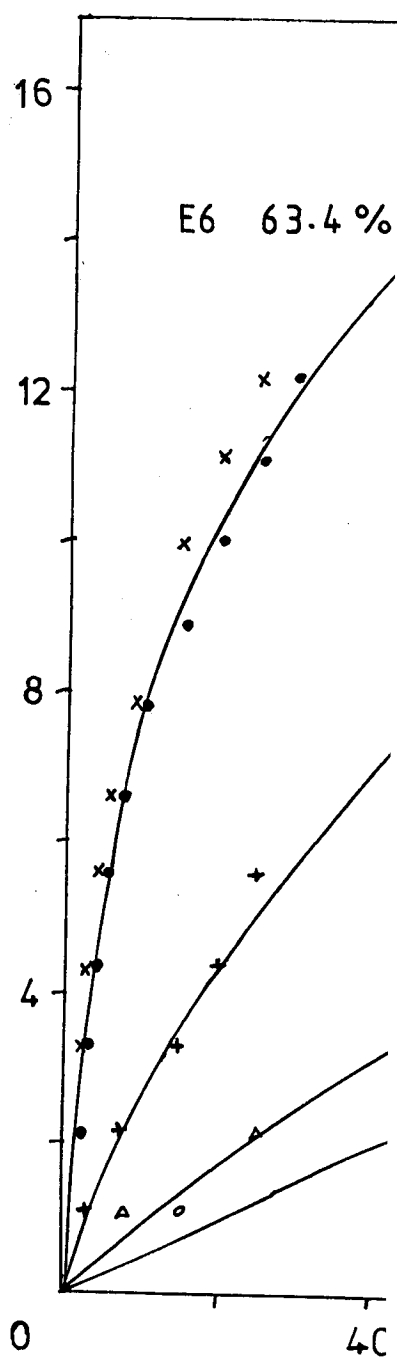
With the other parameters constant, samples were reacted isothermally at six different temperatures between 850 and 1100°C. Figure 14 shows the progress of the reaction with time. At the high temperatures of 1050 and 1100°C the rate of reduction was not significantly increased by the further elevation of temperature. Examination of the physical state of the products showed that samples reacted at 850 and 900°C were not fused and only partially so at 950°C, but appeared completely fused at the higher temperatures of 1050 and 1100°C.

(vi) Dependence of reaction rate on charge porosity

Experiments were carried out under identical conditions save for bulk density of the charge. Three bulk densities of 1.5, 1.7 and 1.9 grams per cm<sup>3</sup> were considered. The results as shown in figure 15 indicate a small increase in the rate of reduction when the void volume of the charge increased.

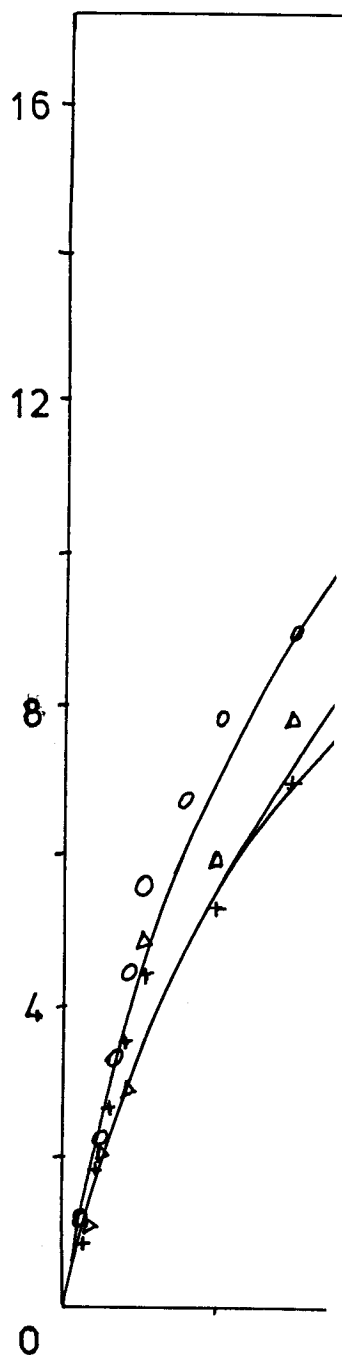
(vii) Effect of lime addition on reaction rate

Figure 16 shows that the addition of lime led to a



(vii) Effect of lime addition on reaction rate

Figure 16 shows that the addition of lime led to a





(vii) Effect of lime addition on reaction rate

Figure 16 shows that the addition of lime led to a reduction in the reaction rate. Whereas a 2.5% lime addition diminished the reaction rate only slightly, a higher CaO content of 5.0% showed a more severe effect.

(B) Degree of cassiterite reduction

Chemical analyses of the reacted samples enabled the degree of  $\text{SnO}_2$  reduction achieved in any particular experiment to be determined. The degree of reduction is reported in Table 8 as:

$$\% \text{ SnO}_2 \text{ reduced} = \frac{(\text{Metallic tin in the product})}{\text{Total tin of the charge}} \times 100$$

The degree of reduction data is also shown along-side the corresponding  $\Delta W_t/W_o$  (%) versus time plots of figure 9 to 16 for ease of comparison. To a fair extent, the degree of  $\text{SnO}_2$  reduction exhibited behaviour akin to that portrayed by the isothermal plots with the possible exception of the results for the addition of lime.

Table 8: Degree of reduction of  $\text{SnO}_2$

Expt. No.	concentrate weight in charge (g)	concentrate % tin	Tin weight in cons (gram)	volume of Iodine titrant ( $\text{cm}^3$ )	tin weight in product (gram) (*)	% S red
B1	0.853	66.9	0.571	27.8	0.168	29.
B2	0.853	66.9	0.571	69.6	0.420	73.
B3	0.831	66.9	0.556	28.4	0.171	30.
B4	0.810	66.9	0.542	39.9	0.241	50.
B5	0.810	66.9	0.542	92.2	0.556	102.
B6	0.737	66.9	0.493	45.6	0.275	55.
B7	0.737	66.9	0.493	103.8	0.626	127.
C <sub>1</sub> = B1	0.853	66.9	0.571	27.8	0.168	29.
C <sub>2</sub>	0.853	66.9	0.571	30.6	0.185	32.
C <sub>3</sub>	0.853	66.9	0.571	26.3	0.159	27.8
D1	0.853	68.2	0.582	22.7	0.137	23.5
D2	0.853	68.2	0.582	56.6	0.341	58.6
D3	0.853	67.5	0.576	19.2	0.116	20.1
D4	0.853	67.5	0.576	44.6	0.269	46.7
D5	0.853	65.8	0.561	18.5	0.112	20.0
E1	0.853	68.2	0.582	13.2	0.080	13.7
E2	0.853	68.2	0.582	23.2	0.140	24.1
E3	0.853	68.2	0.582	31.5	0.190	32.6
E4	0.853	68.2	0.582	53.1	0.320	55.0
E5	0.853	68.2	0.582	60.0	0.362	62.2
E6	0.853	68.2	0.582	61.2	0.369	63.4
F1=E5	0.853	68.2	0.582	60.0	0.362	62.2
F2	0.967	68.2	0.699	65.7	0.396	56.7
F3	1.080	68.2	0.737	69.3	0.418	56.7
G1	0.832	68.2	0.567	18.2	0.110	19.4
G2	0.832	68.2	0.567	63.3	0.382	67.4
G3	0.810	68.2	0.552	55.3	0.333	60.3

Tin equivalent of 0.1N Iodine used was  $6.03 \text{ mg/cm}^3$ .

(C) Composition of exit gas

Data of measured  $\text{CO}_2$  and CO content of evolved gases is summarized in Table 9, in the form of partial pressure ratios  $P_{\text{CO}_2}$  to  $P_{\text{CO}}$ . For each particular experiment, the  $P_{\text{CO}_2}/P_{\text{CO}}$  figure given is an average of measured values, details of which appear in Appendix B.

Table 9:  $\text{CO}_2/\text{CO}$  analysis of product gas

Expt. No.	Temp (°C)	$\text{SnO}_2/\text{C}$ (ratio)	charcoal size (microns)	concentrate size (microns)	Average $P_{\text{CO}_2}/P_{\text{CO}} =$
B3	950	1:1.5	-55	-63	2.33
B4	950	1:2	-55	-63	2.19
B5	1050	1:2	-55	-63	1.78
B6	950	1:4	-55	-63	1.68
B7	1050	1:4	-55	-63	1.18
E1	850	1:1	-106 + 75	-90 + 63	2.71
E2	900	1:1	-106 + 75	-90 + 63	2.64
E3	950	1:1	-106 + 75	-90 + 63	2.42
E4	1000	1:1	-106 + 75	-90 + 63	2.37
E5	1050	1:1	-106 + 75	-90 + 63	2.28
E6	1100	1:1	-106 + 75	-90 + 63	2.25

It is evident from the tabulated data that higher temperature and increased reductant content of the reaction mixture leads to a lower  $P_{\text{CO}_2}/P_{\text{CO}}$  ratio.

## 9. Discussion

### (i) Sources of error

Preceding the discussion of results is a brief mention of the possible sources of experimental error. An idea of these may be helpful in the interpretation of results.

- (a) Balance sensitivity: The balance used for weight loss measurements weighed to the nearest 0.01 gram while reaction samples used were only about 0.90 gram. Thus, even though the weight loss may have occurred continuously this could only be revealed by the balance at a time when the loss had cumulated to a multiple of 0.01 gram. 0.01 gram represents a fairly large fraction of 0.90 gram and it is consequently felt the smoothness of the reported isothermal weight loss data could have been improved had a balance of greater sensitivity been used.
- (b) Iodimetric titration in the presence of much carbon: The black colour of the unreacted carbon had the effect of masking the blue starch-iodine titration end point. The tin content of samples reacted with high carbon ratios were therefore liable to overestimation.
- (c) Gas analysis for carbon monoxide  
Whereas CO<sub>2</sub> absorption was fast and complete, that of CO was laborious and required long times. It has been suggested <sup>29</sup> that CO absorption by acid cuprous chloride solution is never quite complete.

(d) Dissolution of the reaction product

As stated in the experimental procedure, to avoid product loss, the reacted samples were left whilst still in the crucibles to stand for 48 hours in concentrated hydrochloric acid to enable the contents to leach out. Thereafter any material still remaining in the crucible was scraped with an iron wire and added to the beaker which had the dissolved fraction. Determination for tin was then done. Though the scraped material was fine, if any tin was locked within, it could not have been included in the assayed value.

(e) Non-uniformity of samples

The usual uncertainty surrounding sampling has to be mentioned as a possible source of error. Despite corrective steps taken the portion drawn for analysis from a larger bulk may not be quite representative of the latter.

(f) Decomposition of cassiterite prior to tin determination

The decomposition of cassiterite concentrate samples before tin determination was done, as stated earlier, by fusion with a flux mixture of sodium carbonate and borax. By this method, cassiterite decomposition is said <sup>33</sup> to, at best, only approach 95%. The better and more commonly used flux sodium peroxide was unavailable at the time the work was being performed. The tin content of the samples could therefore have been under-stated.

(ii) Temperature effect

Figure 14 revealed that at the high temperatures of 1050 and 1100°C, the rates of reduction were virtually the same.

This would seem to suggest that by about 1050°C the average kinetic energy of reacting molecules has become so high as to have overcome nearly all energy barriers to reaction.

The weight loss monitored in the experiments corresponds to the weight of CO<sub>2</sub> and CO evolved by the reaction of charcoal with cassiterite. Thus at any time, t,

$$\text{total weight loss, } \Delta W_t = W_{\text{CO}_2} + W_{\text{CO}}$$

where:

$$W_{\text{CO}_2} = \text{weight of CO}_2 \text{ lost}$$

and

$$W_{\text{CO}} = \text{weight of CO evolved}$$

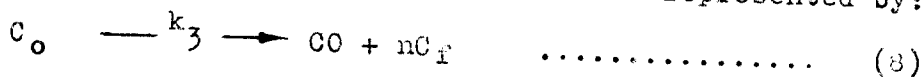
with the further knowledge that  $P_{\text{CO}_2}/P_{\text{CO}} = \alpha$ ,

where  $\alpha$  is a known quantity from gas analysis, it can be shown that the weight of carbon reacted at time, t, to yield CO<sub>2</sub> and CO gases is given by:

$$\Delta W_t^c = \frac{\Delta W_t (0.273\alpha + 0.429)}{1 + \alpha} \dots\dots\dots (14)$$

Derivation of equation (14) is set-out in Appendix 10.

Assuming the rate determining step of the carbothermal reduction of stannic oxide is the reaction represented by:



equation (10) would be expected to describe the kinetics of the reduction,

$$\text{Viz, } -\ln \frac{W_t^c}{W_o^c} = R_c t \dots\dots\dots (10)$$

or

$$\log \frac{W_o^c}{W_t^c} = \frac{R_c}{2.303} t$$

Data obtained in the present work while investigating the influence of temperature on reaction rate has been used in the preparation of Table 10 which shows values of  $\log \frac{W_o^c}{W_t^c}$  at different values of time, t.

The computation of  $W_t^c$  is shown in Appendix 9.

Table 10: Temperature and time dependence data of carbon consumed by reaction with cassiterite.

t reaction time (min)	$\log (W_o^c / W_t^c)$					
	E <sub>1</sub>	E <sub>2</sub>	E <sub>3</sub>	E <sub>4</sub>	E <sub>5</sub>	E <sub>6</sub>
0	0.000	0.000	0.000	0.000	0.000	0.000
1	"	"	"	"	0.0300	0.0300
2	"	"	"	0.0300	0.0630	0.0990
3	"	"	"	0.0300	0.0950	0.138
4	"	"	"	0.0300	0.138	0.138
5	"	"	"	0.0300	0.180	0.182
7.5	"	"	0.0306	0.0630	0.237	0.229
10	"	"	0.0306	0.0630	0.280	0.282
15	"	0.0302	0.0306	0.0950	0.341	0.413
20	"	0.0302	0.0306	0.138	0.413	0.497
25	"	0.0302	0.0633	0.180	0.497	0.601
30	"	0.0302	0.0633	0.180	0.601	0.601
45	"	0.0622	0.0990	0.280	0.739	0.941
60	"	0.0622	0.136	0.339	1.331	1.331
75	0.0302	0.0979	0.136	0.408	1.331	∞
90	0.0302	0.0979	0.179	0.491	∞	∞
105	0.0302	0.1348	0.179	0.491	∞	∞
120	0.0302	0.1348	0.179	0.729	∞	∞
150	0.0302	0.1775	0.226			
180	0.0302	0.2243	0.279			
210	0.0302	0.2243	0.279			
240	0.0622	0.2243	0.279			

The data of Table 10 was used as the basis of the construction of a  $\log (W_o^c/W_t^c)$  versus time plot shown in figure 17.

The plot shows a remarkable linear nature in the early stages of the reaction. This conforms with the expected behaviour of carbon whilst it is oxidised by carbon dioxide. That this should be so in the course of cassiterite reduction lends support to the generally held view that the reaction



determines the overall kinetics of metal oxide ( $MeO_2$ ) reduction by carbon.

Simplification of the equation

$$\frac{-dw^c}{dt} = k_3 W^c (C_o) \dots\dots\dots (9)$$

to obtain equation (10) was based on the assumption that the concentration of occupied sites on the carbon surface remained constant in the early stages of the reaction.

Departure from linearity of the  $\log (W_o^c/W_t^c)$  against time plot can therefore be explained in terms of changes occurring to the active sites on the carbon surface.

For each temperature the slope of the linear portion of figure 17 was used to determine the rate constant,  $R_c$ , of equation 10. These values are tabulated in Table 11.



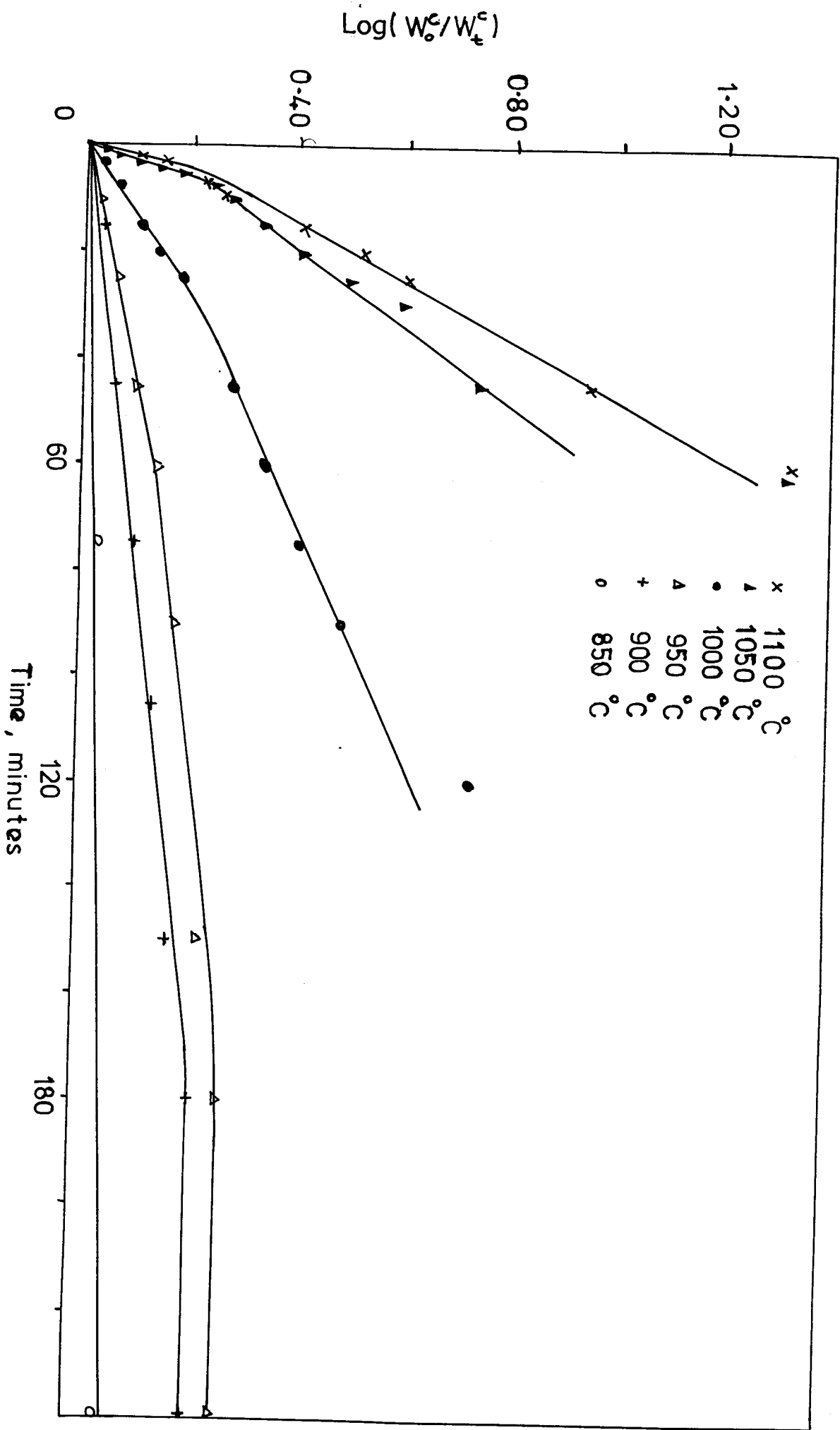


Fig.17: Temp. and time dependence of carbon consumption by reaction with cassiterite

Table 11: Rate constant,  $R_c$ , for the consumption of carbon by reaction with cassiterite.

Temp. (°C)	Temp. T. (K)	$10^{-4}/T$ (K <sup>-1</sup> )	Slope of Fig. 17 $= R_c/2.303$	$R_c$ (min <sup>-1</sup> )	$-\log R_c$
850	1123	8.90	0.00030	0.0069	3.16
900	1173	8.53	0.0013	0.0030	2.52
950	1223	8.18	0.0022	0.0051	2.29
1000	1273	7.86	0.0073	0.017	1.77
1050	1323	7.56	0.036	0.083	1.08
1100	1373	7.28	0.043	0.099	1.00

The rate constant data obtained is shown in Figure 18 as an Arrhenius plot of  $-\log R_c$  against  $1/T$ . Using the slope of the Arrhenius curve, an activation energy of 60.8 kilocalories per mole has been calculated for the consumption of carbon by reaction with cassiterite.

Since the type of carbon and the catalyst action of metals and metal oxides are known to affect the rate of the Boudouard reaction, there is no generally accepted value of the activation energy. However, the value obtained in the present work is quite typical of those found in the literature.

Padilla and Sohn<sup>10</sup> obtained a value of 52.8 kilocalories per mole for the reduction of stannic oxide with coconut charcoal in the temperature range 1073 - 1173 K. Rao and Jalan<sup>23</sup> reported a value of 79.6 kilocalories per mole for the uncatalysed  $\text{CO}_2 + \text{C} = 2\text{CO}$  reaction using porous carbon pellets and pure carbon dioxide while Ergun<sup>25</sup> found a value of 59 kilocalories per mole, for work of a similar nature.

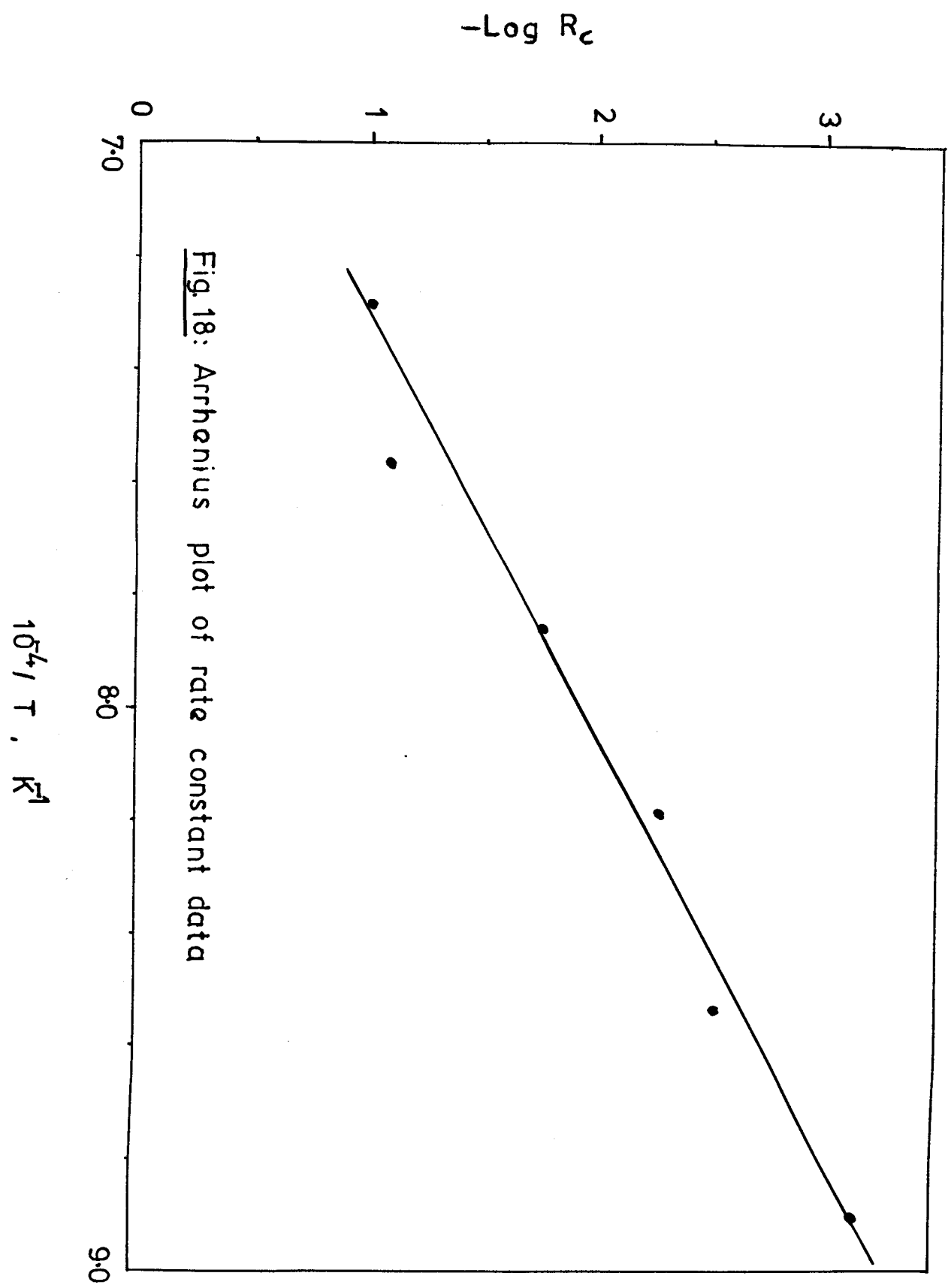
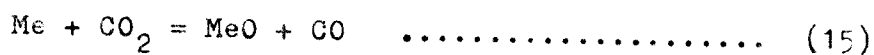


Fig. 18: Arrhenius plot of rate constant data

Indeed, many other values have been found by different researchers. These generally lie in the range 40-97 kilocalories per mole carbon consumed, with the lower values being for catalysed reactions.

Two groups of theories have been used to explain the catalytic action of metals and metal oxides on the Boudonard reaction.

One group centres on a cyclical oxidation - reduction mechanism in which a metal and its oxide participate. Thus, considering a metal Me, such a mechanism can be depicted as :



Alternatively, the catalyst action is explained in terms of an oxygen transfer mechanism involving an oxidation-reduction cycle and electron transfer between  $\pi$  - electrons of graphite and vacant orbitals of the metallic catalyst.

### (iii) Effect of porosity

The method of bulk density change used to study the effect of porosity on the reaction rate did not afford much variation of this parameter.

When the reaction product is not molten, compression of reaction mixtures into discs or pellets enables better study of the porosity effect. As the tin produced by the carbothermal reduction of cassiterite is always molten (melting point,  $232^\circ\text{C}$ ) the use of this method could not be adopted. An attempt could have been made to study pellets held within crucibles had the latter been suitably large.

In the method used, porosity is linked to bulk density by the relation:-

$$\rho_k = \frac{m}{V_T + V_C + V_O} \dots\dots\dots (17)$$

where:  $\rho_k$ , is the bulk density of the charge  
 $m$ , the mass of the charge  
 $V_T$ , the true volume of the charge  
 $V_C$ , the volume of closed voids in the charge  
and  $V_O$ , the open-pore volume of the charge.

Considering the experimental procedure used, it is a reasonable assumption that when the bulk density was changed it was the volume of the open pores of the charge that varied accordingly.

The results therefore show that an increase in the open pore volume of the charge caused an increase in the rate of reaction. This follows from the improved  $CO_2$  and CO transport within the charge.

(iv) Concentrate particle size

The decrease in the rate of reaction with increased particle size of the concentrate can be explained in terms of the reduced surface area of  $SnO_2$  available for reaction with the produced CO.

(v) Charcoal particle size

The assumption that the reaction on the carbon surface is rate controlling also explains the influence of charcoal particle size on the cassiterite - charcoal reaction.

Due to the porous nature of carbon, even inner regions are readily available for reaction with carbon dioxide to form carbon monoxide. The reaction rate is therefore not dependent on external surface area as represented by the particle size.

The size range investigated was up to 150 microns because of the crucible and reactor size limitation. It is possible however, that this behaviour may have held even up to larger charcoal particle sizes. Ergun<sup>25</sup> found that the oxidation of carbon particles in a CO<sub>2</sub> stream was independent of the particle size in the range 0.08 mm to 1.8 mm.

(vi) Relative amounts of charcoal and cassiterite

The increase in reduction rate caused by larger contents of carbon in the reaction mixture can be attributed to the increase in the velocity of the rate controlling reaction



whose rate, as was stated before, depends on the concentration (C<sub>o</sub>) in the charge.

(vii) Effect of lime addition

The weight loss data showed that addition of lime led to a reduction in the reaction rate, slightly at low CaO contents and more strongly for higher amounts. It seems this behaviour could have been caused by charge porosity diminution, in view of the fineness of the lime used.

When the degree of  $\text{SnO}_2$  reduction achieved in the experiments is considered, the overall effect of lime addition is not so straight forward at high temperature.

At low temperature a clear decrease in the degree of  $\text{SnO}_2$  reduction supports the view that the reaction rate was minimised by lime addition.

At high temperature a 5% rise in the degree of  $\text{SnO}_2$  reduction was noted with an addition of 2.5%  $\text{CaO}$ .

It appears, whereas the reaction rate was minimised, the time allowed was long enough for the sample to have reached the same extent of reaction completion as the equivalent ordinary cassiterite plus charcoal mixture. This being the case, unless  $\text{CaO}$  interfered with iodimetric titration of tin, which is considered highly unlikely as no mention is found in the literature, the lime content must have acted to produce a product which had tin in a more readily assayable form. This could, for instance, arise if the molten non-metallic part of the product and the tin drops formed were rendered immiscible.

(viii) Gas composition

The gas composition determined in the various experiments is presented in Table 12 as  $\log (P_{\text{CO}_2}/P_{\text{CO}})$ . That the rate of carbon dioxide reaction on the carbon surface is faster at higher temperatures and higher charcoal contents of the samples, can be seen from the consequent reduction in the  $P_{\text{CO}_2}$  to  $P_{\text{CO}}$  ratios.

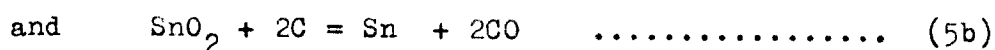
Table 12: Composition of exit gas

Expt. No.	Temp., T. (°C)	T (K)	1000/T (K <sup>-1</sup> )	P <sub>CO<sub>2</sub></sub> /P <sub>CO</sub>	log(P <sub>CO<sub>2</sub></sub> /P <sub>CO</sub> )
E1	850	1123	0.89	2.71	0.43
E2	900	1173	0.85	2.64	0.42
E3	950	1223	0.82	2.42	0.38
E4	1000	1273	0.79	2.37	0.37
E5	1050	1323	0.76	2.28	0.36
E6	1100	1373	0.73	2.25	0.35
B3	950	1223	0.82	2.33	0.37
B4	950	1223	0.82	1.38	0.34
B5	1050	1323	0.76	1.78	0.25
B6	950	1223	0.82	1.68	0.23
B7	1050	1323	0.76	1.18	0.07

The measured gas compositions are plotted with (x) marks on Figure 2. All are in the region of Sn<sub>(l)</sub> and FeO<sub>(s)</sub> stability, regardless of whether the activities of Sn and FeO decrease from unity to lower values. It would have been of interest to have examined in what form the iron occurred in the reacted samples by XRD analysis had facilities permitted.

(ix) Degree of SnO<sub>2</sub> reduction

As discussed earlier, the reactions





do not indicate the mechanism by which the reduction of cassiterite occurs. Nevertheless, for thermodynamic analysis which only depends on the initial and final states of the system under study, the two equations can be used to compute the amount of tin produced in any particular experiment.

It can be shown (Appendix 10) that the weight of tin produced is given by:

$$W_{sn} = \frac{\Delta W}{1 + \alpha} (2.697\alpha + 2.119) \dots\dots\dots (18)$$

where  $\Delta W$  = total weight loss of the sample.

and  $\alpha = P_{CO_2}/P_{CO}$ .

Tin contents calculated with the aid of equation (18) are compared with those obtained by iodimetric titration in Table 13.

Table 13: Comparison of calculated and chemically determined amounts of tin produced.

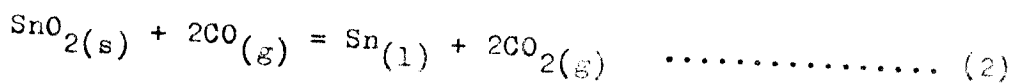
Expt No.	$\alpha$	$\Delta W$ (gram)	$W_{sn}$ (gram)	Analysed Sn (gram)	% Difference relative to analysis
B3	2.33	0.07	0.177	0.171	+3.5
B4	2.19	0.09	0.226	0.241	-6.2
B5	1.78	0.22	0.548	0.556	-1.4
B6	1.68	0.11	0.273	0.275	-0.7
B7	1.18	0.26	1.378	0.626	+351.6
E1	2.71	0.02	0.051	0.080	- 36.3
E2	2.64	0.06	0.152	0.140	+ 8.6
E3	2.42	0.07	0.177	0.190	- 6.8
E4	2.37	0.12	0.303	0.320	- 5.3
E5	2.28	0.15	0.378	0.362	+ 4.4
E6	2.25	0.15	0.378	0.369	+ 2.4

Reasonable agreement can be seen in all cases except two. No explanation can be offered as to the cause of the smaller of the anomalies, other than to suggest that the sample weight loss was much too small so that the effect of any errors would appear magnified. The sample with the extraordinary difference was with a very high carbon content ( $\text{SnO}_2/\text{C} = 1/4$ ) and was reacted at a high temperature ( $1050^\circ\text{C}$ ). It would be reasonable to believe that a large part of the difference between the calculated tin content of the product and that analysed originated from reduced iron oxides. The effect of such reduction would be to give a higher weight loss value than would have been obtained otherwise.

### CHAPTER THREE: REDUCTION BY CARBON MONOXIDE

#### 10. Theory: Obtaining kinetic data

In the absence of carbon,  $\text{SnO}_2$  is reduced by carbon monoxide according to the equation:

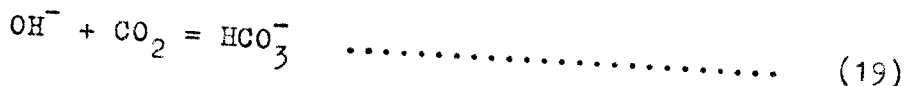


When pure carbon monoxide is used as the reductant, the off-gas from the reaction vessel would consist of carbon dioxide and unutilised carbon monoxide.

The solubility of carbon monoxide in KOH solution at room temperature is negligible whereas that of carbon dioxide is considerable.

If the off-gas from the reaction vessel was therefore bubbled through a KOH solution, it would be possible to determine the rate of the reaction represented by equation (2). This would be achieved by considering the increment in weight of the solution, caused by  $\text{CO}_2$  absorption, as a function of time. A version of this method was cited earlier as having been used by Srinivasan and Lahiri<sup>4</sup> and Hopkins and Adlington<sup>3</sup> in determining  $P_{\text{CO}_2}$ . Due to the minute weight changes dealt with in the present study, this method could not be adopted.

Absorption of  $\text{CO}_2$  in KOH solution could still however be used as the basis for determining the rate of cassiterite reduction by carbon monoxide. Dissolution of the carbon dioxide leads to a consumption of hydroxyl anions and consequently causes a decrease in the pH of the KOH solution. The dissolution can be represented by:-



The pH of a solution is defined as,  $\text{pH} = -\log a_{\text{H}^+}$ . In aqueous solutions, the product of  $\text{H}^+$  and  $\text{OH}^-$  ion concentrations is a constant at a particular temperature. This means that though it is  $\text{OH}^-$  anions that are depleted in a KOH solution by reaction with  $\text{CO}_2$  the discussion can still be made in terms of  $\text{H}^+$  ions.

The pH can be further expressed as:-

$$\text{pH} = -\log C_{\text{H}^+} \cdot \gamma_{\text{H}^+} \dots\dots\dots (20)$$

where:  $C_{\text{H}^+}$  = concentration of  $\text{H}^+$  ions

and  $\gamma_{\text{H}^+}$  = activity coefficient of  $\text{H}^+$  ions

In aqueous solutions of low ionic strength, the value of the activity coefficient  $\gamma_{\text{H}^+}$  can be obtained by use of the Debye-Huckel equation

$$-\log \gamma_{\text{H}^+} = \frac{AZ^2 \sqrt{I}}{1 + B \bar{a} \sqrt{I}} \dots\dots\dots (21)$$

where: (i) Z is the ionic charge; for  $\text{H}^+$ ,  $Z = 1$

(ii) I is the ionic strength and is given by the relation  $I = \frac{1}{2} \sum C_i Z_i^2$ , the summation being extended over all the ions in solution.

(iii) A and B are Debye-Huckel constants, and are functions of temperature and dielectric constant of the solvent. Values of A and B for the aqueous medium can be read from tables<sup>34</sup>.

and (iv)  $\bar{a}$  is the ion size parameter for which 5 Angstrom can be taken as an average<sup>35</sup>.

For a known value of pH, it is therefore possible to compute the hydrogen ion concentration by use of the relation.

$$-\log C_{\text{H}^+} = \text{pH} - \frac{AZ_{\text{H}^+}^2 \sqrt{I}}{1 + B \bar{a} \sqrt{I}} \dots\dots\dots (22)$$

If the pH changed to another value, the corresponding  $H^+$  concentration would again be similarly evaluated. With the further knowledge of the volume of the absorbing solution the amount of  $CO_2$  needed to cause the pH change could be calculated.

By observing the rate of change in pH of caustic potash solution caused by the dissolution of  $CO_2$ , the progress of the reaction represented by equation (3) could be monitored. In the present work this method was used to study the kinetics of the  $SnO_2 + CO$  reaction.

An obvious drawback of this method is that, with time, dissolution of  $CO_2$  occurs in KOH solution of diminishing strength. On the other hand too high concentrations of KOH solution would not permit detection of concentration changes caused by dissolution of small amounts of  $CO_2$ .

These problems could be alleviated by conducting the experiment with KOH solution of moderate concentration and arranging that the experiment ends before  $OH^-$  concentration is too low. In the experiments performed, 0.005 M KOH was used and the end was signified by the fall in pH to a value of 10.

## 11. Apparatus

The apparatus used for the reduction of cassiterite concentrate by carbon monoxide is shown in figure 19.

It comprised of a hot-plate (1) on which was placed a 500 ml erlenmeyer flask (2) fitted with a three holed rubber stopper. One hole of the stopper facilitated the provision of nitrogen gas to the flask while another was for gas removal. A burette (3) clamped vertically above the flask, had its tip inserted into the third hole.

During the course of the experiment, the flask contained hot concentrated sulphuric acid while the burette was filled with formic acid.

Exit gas from the erlenmeyer flask was dried in a silica gel column (4) before being introduced into a silica tube (5) which was centrally positioned in a horizontal tube furnace (6).

The silica tube also had a facility of being flushed with nitrogen gas.

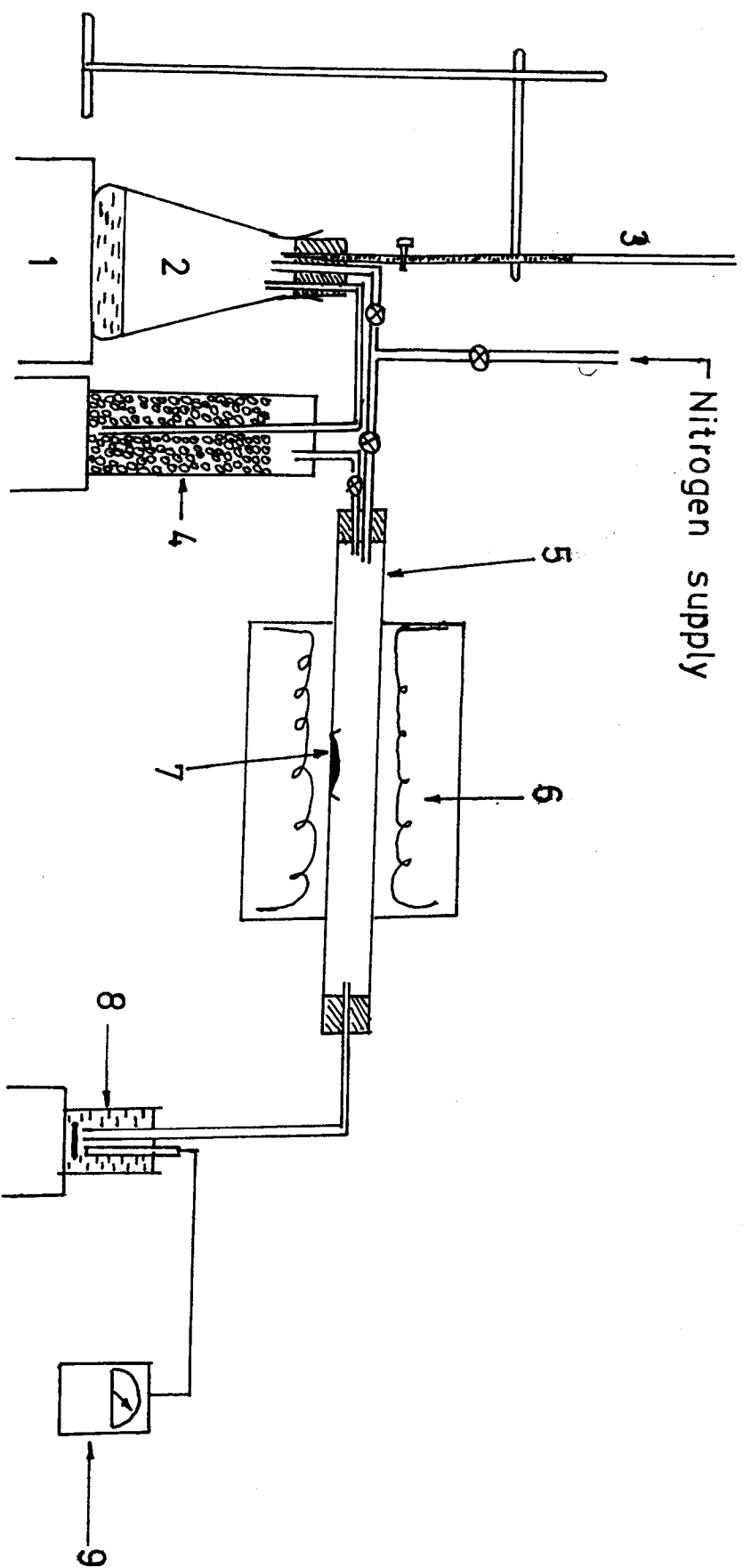
An alumina boat (7) contained the cassiterite sample for reduction and it was placed inside the silica tube at the centre of the furnace.

Gases emerging from the silica tube were bubbled through a magnetically stirred KOH solution (8) of known concentration and temperature. Dipping into the KOH solution was an electrode of a pH meter (9) which was used to monitor the acidity of the solution.

The whole experimental assembly was installed in a fume cup-board.

- 1 Hot plate
- 2 Flask with conc.  $\text{H}_2\text{SO}_4$
- 3 Burette with formic acid
- 4 Silica gel column
- 5 Silica tube

- 6 Tube furnace
- 7 Sample boat
- 8 Magnetically stirred KOH soln.
- 9 pH meter



## 12. (a) Experimental procedure

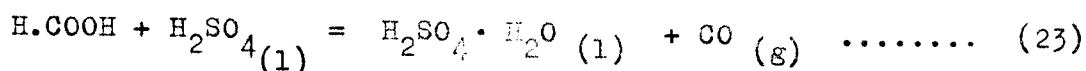
0.5000 gram of -90 to + 63 micron cassiterite concentrate was weighed into an alumina boat of known weight. The concentrate was spread out to form a very thin layer before the boat was pushed into position inside the silica tube.

150 millimetres of concentrated sulphuric acid, a volume well in excess of requirement, was put into the erlenmeyer flask while the burette was filled with 20 cm<sup>3</sup> of formic acid. The H<sub>2</sub>SO<sub>4</sub> was heated to about 100°C and maintained at this temperature.

The apparatus was then linked up as shown in figure 19. All fittings were gas tight. Rubber tubing clips were loosened and a low nitrogen flow was made to displace air from the erlenmeyer flask and silica tube. Following this, the furnace was switched on and allowed to heat up to the working temperature. Once this was attained and a further 15 minutes had elapsed, the nitrogen flow was stopped and the clips on the nitrogen supply tubing screwed tight.

Formic acid was then allowed to trickle onto the hot concentrated sulphuric acid at a rate of about one drop every 5 seconds.

Contact between the two acids immediately produced bubbles of carbon monoxide according to the reaction <sup>36</sup>



After being dried in the silica gel column, this gas then passed over the alumina crucible containing the cassiterite sample. The exit gas from this section was bubbled through 150 cm<sup>3</sup> of potassium hydroxide solution whose pH and temperature were periodically monitored.



At the end of the experiment, that is, when the pH had decreased from 11.9 to 10.0, the furnace was switched off and the flow of nitrogen through the reactor was resumed. Carbon monoxide flow was at the same time stopped by use of a clip on the supply tubing before removing the erlenmeyer flask from the experimental assembly. The sample boat was then allowed to cool to near room temperature. After this, the nitrogen flow was stopped and the alumina boat removed. The boat was later weighed to establish the weight loss sustained by the sample.

The next step was the iodimetric titration for metallic tin contained in the reacted product. Preparation for, and actual analysis were done in a manner similar to that used for the carbothermally reduced products.

(b) Experimental schedule

The experiments done, whose only variable was the reaction temperature, are listed in Table 14.

Table 14: Experimental schedule

Expt. No.	Temp. (°C)	Concentrate size (microns)
H1	900	-90 + 63
H2	950	"
H3	1000	"
H4	1050	"
H5	1100	"

### 13. Results

#### (i) Variation of pH with reaction time

The pH values recorded in the experiments performed are shown in Table 15. In all cases the KOH solution temperature was between 19 and 20°C.

Table 15: pH of KOH as a function of reaction time

Time (mins)	pH values				
	H1	H2	H3	H4	H5
0	11.9	11.9	11.9	11.9	11.9
1	11.9	11.9	11.85	11.8	11.8
2	11.9	11.85	11.8	11.7	11.65
3	11.9	11.8	11.75	11.55	11.5
4	11.9	11.8	11.7	11.45	11.4
5	11.85	11.75	11.6	11.4	11.3
7.5	11.8	11.65	11.45	11.2	10.9
10	11.75	11.55	11.3	10.8	10.0
12.5	11.7	11.45	11.15	10.0	
15	11.65	11.35	10.9		
19			10.0		
20	11.6	11.1			
25	11.5	10.6			
27		10.0			
30	11.25				
35	10.85				
38	10.0				

(ii) Sample weight loss data

The initial and final weights of the alumina boat plus contained sample for each experiment are presented in Table 16. The table also shows the weight of tin formed calculated on the basis of sample weight loss and stoichiometry of the  $\text{SnO}_2 + \text{CO}$  reaction. Details of the calculation appear in appendix 12.

Table 16: Weight of tin formed as calculated from sample weight loss data

Expt. No.	Total initial weight (mg)	Total final weight (mg)	Weight loss (mg)	Weight tin formed (mg)
H1	950.0	938.8	11.2	41.5
H2	769.3	757.8	11.5	42.7
H3	604.7	593.4	11.3	41.9
H4	785.4	773.7	11.7	43.4
H5	768.2	756.6	11.6	43.0

(iii) Iodimetric titration

The HCl dissolved reaction products were titrated against iodine for contained tin. Standardisation of the titrant showed its tin equivalent was  $6.03 \text{ mg Sn per cm}^3$ . Results of the titration appear in Table 17.

Table 17: Weight of metallic tin in reacted samples (by chemical analysis)

Experiment No.	Volume Iodine (cm <sup>3</sup> )	Tin Content (mg)
H1	7.5	45.2
H2	7.8	47.0
H3	6.9	41.6
H4	7.0	42.2
H5	6.7	40.4

# 14. Discussion

## (i) Content of metallic tin in reacted samples

The pH data of Table 15 was converted by a series of calculations, details of which appear in Appendix 11, to show the cumulative weight of tin formed as a function of time. The cumulative weight of tin appears in Table 13.

Table 13: Cumulative weight of tin formed as a function of time.

Time (Min.)	Tin formed, $m_{\text{Sn}}$ (mg)				
	H1	H2	H3	H4	H5
0	0	0	0	0	0
1			4.75	8.90	8.90
2		4.75	9.40	16.62	19.50
3		8.90	13.06	24.33	26.71
4			16.62	28.49	30.27
5	4.75	13.06	21.26	30.27	33.23
7.5	8.90	19.50	28.49	35.61	40.06
10	13.06	24.33	33.23	40.95	43.97
12.5	16.62	28.49	36.75	43.97	
15	19.50	32.05	40.06		
19			43.97		
20	21.96	37.39			
25	26.71	42.25			
27		43.97			
30	34.42				
35	40.47				
38	43.97				

This difficulty was not possible for experiments conducted at the higher temperatures and could have been the cause of the rather low values of tin content obtained by chemical analysis.

It should be noted that the metallic tin content of the product as determined at the end of the experiment does not necessarily correspond to that which would be obtainable under conditions of maximum  $\text{SnO}_2$  reduction by CO. Due to experimental limitations stated earlier the reaction was stopped when the value of the absorbant solution decreased to a value of 10.0.

(ii) Rate of tin formation

Table 18 which shows the cumulative weight of tin formed as a function of time was used to draw up Table 20. This table shows the cumulative weight of metallic tin formed,  $\text{Sn}_t$ , up to any time (t) as a percentage of the total tin contained in the unreduced  $\text{SnO}_2$  sample.

(iii) Temperature dependence of reaction rate

From figure 20 it can be seen that an increase in reaction temperature leads to higher reaction rate. This follows from considerations of the proportion of reacting molecules that are, at any temperature, in possession of kinetic energy greater than the activation energy,  $E_A$ . The Maxwell-Boltzmann energy distribution law gives the number of molecules with energy greater than  $E_A$  as being proportional to  $\exp(-E_A/RT)$ . Thus an increase in temperature should raise the reaction rate.

Table 20: Cumulative weight of tin added as a percentage of total tin contained.

Time (Min.)	$\text{Sn}_t/\text{Sn}_0$ (%)				
	H1	H2	H3	H4	H5
0	0	0	0	0	0
1			1.4	2.6	2.6
2		1.4	2.6	4.9	5.7
3		2.6	3.8	7.1	7.8
4			4.9	9.4	9.7
5	1.4	3.8	6.4	10.9	11.7
7.5	2.6	5.7	8.4	12.0	12.9
10	3.8	7.1	9.7	12.9	
12.5	4.9	8.4	10.9		
15	5.7	9.4	11.7		
19			12.9		
20	6.4	11.0			
25	7.8	12.4			
27		12.9			
30	10.1				
35	11.9				
38	12.9				

The data of Table 20 was then used as the basis for Figure 20, a plot of  $\text{Sn}_t/\text{Sn}_0$  (%) against time, with temperature as a second variable.

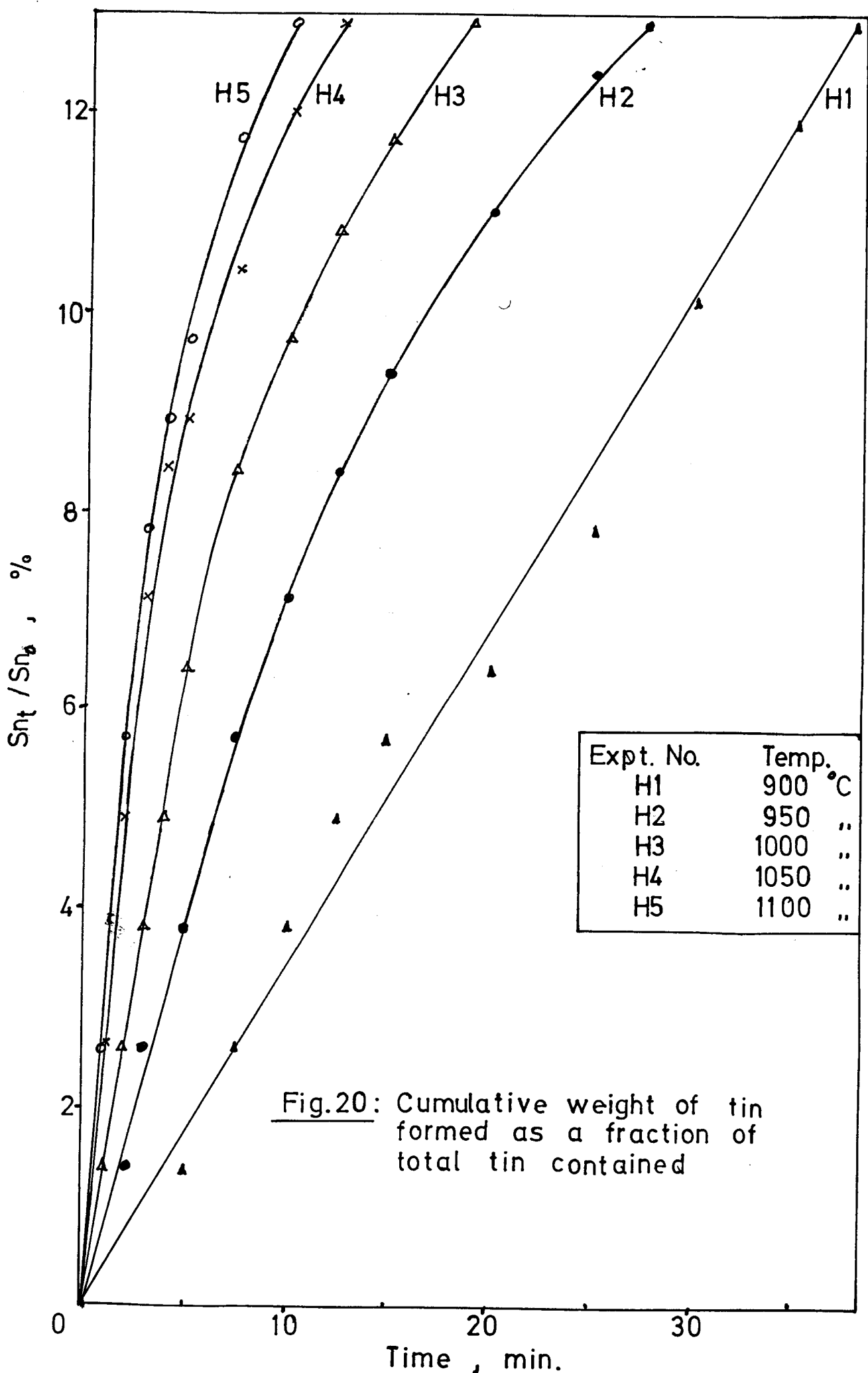




Figure 20 further shows that the initial stages of the  $\text{SnO}_2 - \text{CO}$  reaction occurred at a constant reaction rate. This phenomenon may be interpreted by considering the processes that could be regarded as constituting the reaction. Under the experimental conditions used, these processes are:-

- (a) transport of CO to the reaction site
- (b) the  $\text{SnO}_2 - \text{CO}$  interface reaction, which in itself also consists of adsorption of CO, the  $\text{SnO}_2 - \text{CO}$  reaction proper, as well as the desorption of  $\text{CO}_2$ .
- (c) diffusion of  $\text{CO}_2$  away from the reaction site.

At the very beginning of the experiment, steps (a) and (c) would be expected to be of negligible influence on the reaction rate. Hence step (b) would govern the course of reduction. During this initial period so little of the  $\text{SnO}_2$  would have been used up that its concentration would be virtually constant. The rate of the interface reaction (b) would therefore also be virtually constant since the rate of a reaction is defined in terms of the rate of change of concentration. The addition rate of formic acid to concentrated sulphuric acid was, despite its intermittent manner, sufficient to at all times ensure rapid production of CO in amounts well in excess of reaction requirement.

The duration of constant reaction rate was about 2 minutes at  $1100^\circ\text{C}$  and progressively longer at lower reaction temperatures. It is possible in all cases that such times could have been longer but, as stated earlier, absorption of  $\text{CO}_2$  occurred into a KOH solution of diminishing strength.

for each experiment, the initial reaction rate,  $R_i$ , was evaluated as the slope of the linear section of the corresponding curve in Figure 20. These rates were used in estimating the energy requirements of the  $\text{SnO}_2 + \text{CO}$  reaction. Table 21 shows the initial rates so evaluated and associated data needed for the Arrhenius plot of Figure 21.

Table 21: Temperature dependence of initial reaction rates

Expt. No.	Temp ( $^{\circ}\text{C}$ )	Temp., T (K)	$10^{-4}/T$ ( $\text{K}^{-1}$ )	Initial rate $R_i$ ( $\text{min}^{-1}$ )	$\log R_i$
H1	900	1173	8.53	0.034	-2.47
H2	950	1223	8.18	0.076	-2.12
H3	1000	1273	7.86	0.213	-1.89
H4	1050	1323	7.56	0.324	-1.62
H5	1100	1373	7.28	0.551	-1.51

Two straight lines could each fit the data of Figure 21 adequately. Using the slopes of these lines, the activation energy for the  $\text{SnO}_2 + \text{CO}$  reaction was estimated to be between 31.0 and 40.1 kilocalories per mole ~~of~~ formed.

This result further supports the notion that in the  $\text{SnO}_2 + \text{carbon}$  reaction scheme represented by :-



the slow step is reaction (3) for which the activation energy requirement of 60.8 kilocalories per mole carbon consumed, found earlier, is much larger than that determined for reaction (2).

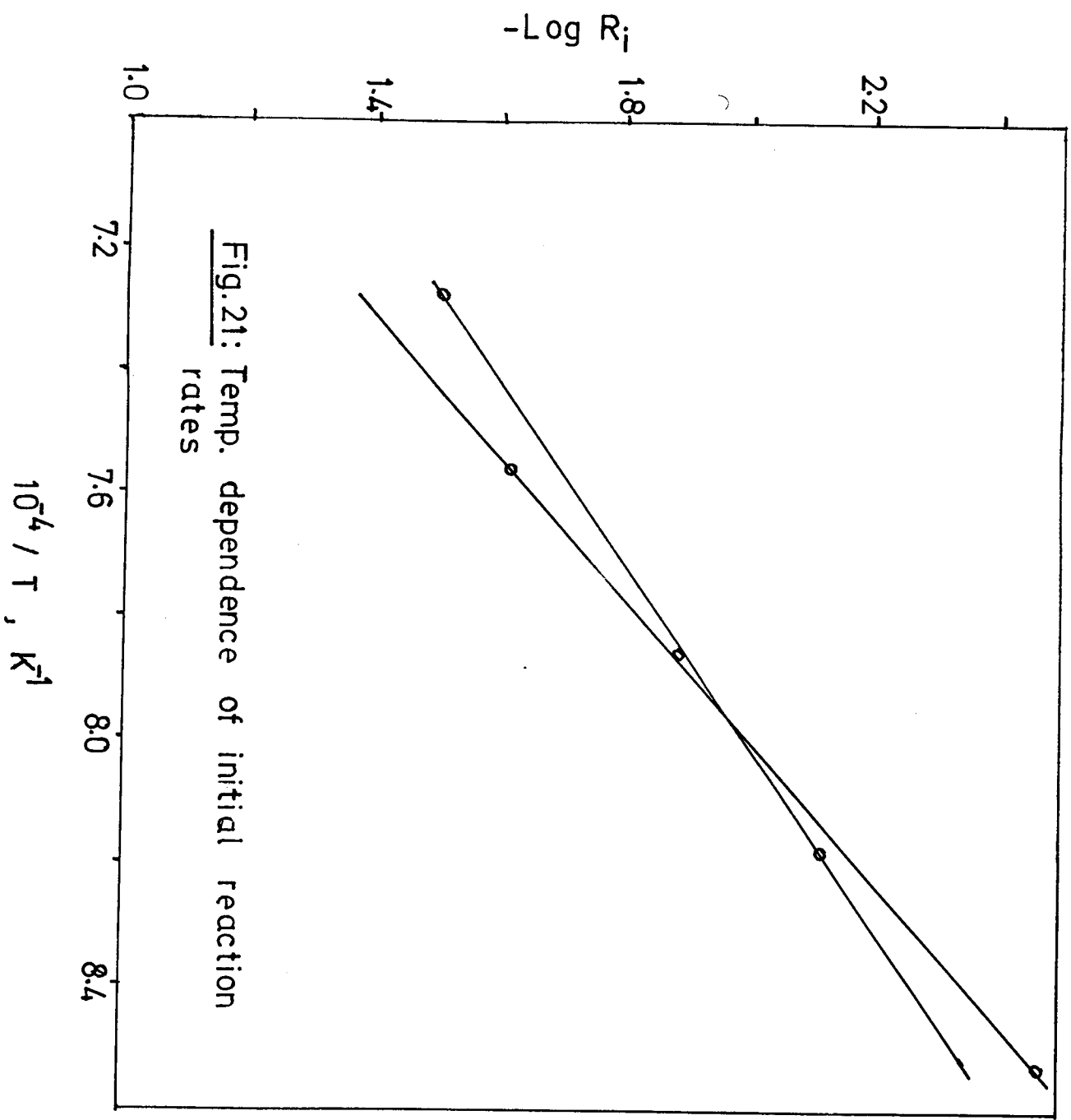
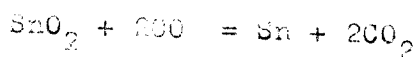


Fig.21: Temp. dependence of initial reaction rates

#### CHAPTER FOUR: CONCLUSIONS

Cassiterite is readily reduced to tin metal by charcoal. The reaction was found to commence at about 950°C, but its rate only reached an appreciable extent between 1000 and 1050°C. Improvement in the reduction rate by further increase in temperature was found insignificant. At 950 and 900°C the product of reduction was not fused, and was only partially so at 950°C, but appeared completely fused at the higher temperatures of 1050 and 1100°C.

Kinetic data obtained from isothermal experiments was found consistent with the assumption that in the two step carbothermal reduction mechanism of  $\text{SnO}_2$  denoted by:-



the latter reaction is rate controlling for which an activation energy of 60.3 kilocalories per mole was determined. The relative ease of the  $\text{SnO}_2 + \text{CO}$  reaction was reflected in the lower mean activation energy value found of about 35.6 kilocalories per mole tin formed.

Besides temperature, the proportion of charcoal in the reaction mixture was also found to have an important effect on the cassiterite reduction rate. Higher charcoal contents led to faster reaction rates.

A combination of high temperature and charcoal proportions was in particular found to be of synergic influence on the rate. This combination however, especially with excessive reductant, may have caused reduction of other oxides present in the sample.

Under all experimental conditions considered, tin and composition indicated  $\text{SnO}_2$  and  $\text{Fe}_2\text{O}_3$  in the concentrate were reduced to Sn and Fe respectively. Chemical analysis confirmed the presence of metallic tin in the product.

Whereas the rate of reduction was independent of charcoal particle size (investigated up to 150 microns) increased cassiterite particle size diminished it.

It was further found that the reduction of more porous charge mixtures proceeded faster than those with less void space.

High temperature reaction of charge mixtures with an addition of 2.5% lime was found to result in a better tin product.

Finally, it may be stated that cassiterite would be best reduced with a combination of:

- high temperature
- reasonably high charcoal proportions
- high charge porosity
- fine cassiterite size
- and addition of a small percentage of lime.

References

1. Mantell, C.L., Tin, Butter, New York, 1970
2. Wright, P.A., Extractive metallurgy of tin, Elsevier, Amsterdam, 1966.
3. Hopkins, D.W., and Allington, A.G., factors affecting the reduction of zinc oxide by carbon, Trans. IMM, 60, 1951, 101 - 116.
4. Srinivasan, M.S., and Lalini, A.K., studies on the reduction of hematite by carbon, Metall. Trans., 6B, 1977, 175-178.
5. Rao, Y.K., the kinetics of reduction of hematite by carbon, Metall. Trans., 1971, 2, 1439 - 1447.
6. Maru, Y., et al., kinetic studies of the reaction between  $\text{Cr}_{23}\text{C}_6$  particles and  $\text{Cr}_2\text{O}_3$  particles, Metall. Trans., 1973, 4, 2591 - 2598.
7. Lin, I.J., and Rao, Y.K., Reduction of lead oxide by carbon, Trans. IMM, 84, 1975, 876-82.
8. Truehan, R.J., the rate of reduction of iron oxides by carbon, Metall. Trans., 10B, 1977, 279 - 286.
9. Rankin, W.J., reduction of chromite by graphite and carbon monoxide, Trans. IMM, 7, 1978, 0180-183.
10. Padilla, R., and Sohn, H.Y., the reduction of stannic oxide with carbon, Metall. Trans., 10B, 1979, 109 - 115.
11. Legg, C.A., The tin belt of southern province, Geological Survey of Zambia, Econ. rep., 21, 1972, 45.
12. Ibid., 8 - 12.

14. Central Statistical Office, Year Books:  
Statistics of Industrial production, 1982/3.
15. Standen, A., Ed., Knaul-Othmer encyclopedia of chemical  
technology, Interscience, New York, 1969, 20, 277
16. Kubaschewski, O., and Alcock, C.B.,  
Metallurgical thermochemistry, Pergamon, Oxford, 1979.
17. Coughlin, J.P., U.S. Bureau of Mines  
Bull. No. 542, 1954.
18. Rosenqvist, P., Principles of extractive metallurgy,  
McGraw-Hill, Tokyo, 1974, 268.
19. Hulett, J.R., Deviations from the Arrhenius equation,  
Quarterly reviews of Chem. Soc., 18, 1964, 227.
20. Moore, J.J., et al., Chemical metallurgy,  
Butterworths, London, 1981, 113 - 115.
21. Levin, E.M., and McMullin H.R., Eds.,  
Phase diagrams for ceramists, American ceramic society,  
New York, 1964, 204.
22. Findlay, A., The phase rule and its applications,  
Dover, New York, 1951, 15.
23. Rao, Y.K., and Jalan, B.P., A study of the rates of carbon -  
carbon dioxide reaction in the temperature range 839 - 1050°C,  
Metall. Trans., 3, 1972, 2465 - 2477.
24. Walker, P.L. Jr., Ed., Chemistry and physics of carbon,  
Edward Arnold, London, 1965, 210.
25. Ergun, S., Kinetics of the reaction of carbon dioxide with  
carbon, J. Phys. Chem., 60, 1956, 480 - 485.

26. Walker, P.L. Jr., M.Sc., Chemistry and Physics of carbon, Edward Arnold, London, 1965, 217.
27. Sevryukov, N., et al., General metallurgy, Mir, Moscow, 1969, 279.
28. Floyd, J.M., and Corns, D.S., Reduction of liquid iron smelting slags, Trans. Instn. Min. Engrs., 1979, C111 - 122.
29. Vogel, A.I., A text-book of quantitative Inorganic analysis, Longmans, London, 1961, 1061-1083.
30. Donaldson, E.M., Methods for the analysis of ores, rocks and related materials, Energy, Mines and resources, Ottawa, 1982, 525-528.
31. Dee Snell, F., Ed., Encyclopedia of Industrial Chemical analysis, Interscience, New York, 1974, 19, 42-47.
32. Dolezal, J., Decomposition techniques in inorganic analysis, Iliffe, London, 1968, 16.
33. Ibid., pp 95.
34. Bates, R.G., Determination of pH - theory and practice, Wiley, New York, 1964, 406.
35. Albert, A., and Serjeant, E.P., Ionisation constants of acids and bases - a laboratory manual, Methuen, London, 1962, 58.
36. Mellor, J.W., Comprehensive treatise on inorganic and theoretical chemistry, Longman, London, 1961, V, 911.



## A P P E N D I C E

1. Weight loss data for experiments A1 and A2.
2. Data for experiments B1 to B7.
3. Data for experiments C1 to C3.
4. Results for experiments D1 to D5.
5. Results for experiments E1 to E6.
6. Data on porosity experiments
7. Data on the effect of lime addition.
8.  $\text{CO}_2/\text{CO}$  content of exit gas.
9. Data for the kinetic analysis of temperature effect.
10. Derivation of the equations for the extent of carbon burn-off and amount of tin produced.
11. Reduction of cassiterite concentrate by carbon monoxide: sample calculations.
12. Calculation of tin content of reacted samples from sample weight loss data.

APPENDIX 2:

(a) Experiments B1 to B7: Variation of weight with time

Reaction time (Min)	Sample weight (gram)						
	B1	B2	B3	B4	B5	B6	B7
0	0.90	0.90	0.90	0.90	0.90	0.90	0.90
1	0.90	0.89	0.90	0.90	0.85	0.90	0.83
2	0.90	0.89	0.90	0.90	0.84	0.89	0.78
3	0.90	0.86	0.90	0.89	0.83	0.89	0.75
4	0.90	0.85	0.90	0.89	0.81	0.89	0.73
5	0.90	0.84	0.89	0.89	0.79	0.88	0.71
7.5	0.89	0.84	0.89	0.88	0.76	0.87	0.68
10	0.89	0.81	0.89	0.88	0.74	0.86	0.66
15	0.88	0.79	0.88	0.87	0.70	0.86	0.64
20	0.88	0.78	0.87	0.86	0.69	0.85	0.64
25	0.88	0.77	0.87	0.86	0.68	0.84	0.64
30	0.87	0.76	0.87	0.85	0.68	0.83	0.64
45	0.86	0.76	0.85	0.84	0.68	0.82	
60	0.86	0.75	0.85	0.83	0.68	0.81	
75	0.85	0.75	0.84	0.83	0.68	0.80	
90	0.85	0.75	0.84	0.82	0.68	0.79	
105	0.84	0.75	0.83	0.82		0.78	
120	0.84	0.75	0.83	0.81		0.78	

# APPENDIX 3

## Experiments C1 to C3: Weight loss data

Reaction time (Min)	C1=B1	C2			C3		
	$\frac{\Delta W_t}{W_o} (\%)$	$W_t (g)$	$\Delta W_t (g)$	$\frac{\Delta W_t}{W_o} (\%)$	$W_t (g)$	$\Delta W_t (g)$	$\frac{\Delta W_t}{W_o} (\%)$
0	0.0	0.90	0.00	0.0	0.90	0.00	0.0
1	0.0	0.90	0.00	0.0	0.90	0.00	0.0
2	0.0	0.90	0.00	0.0	0.90	0.00	0.0
3	0.0	0.90	0.00	0.0	0.90	0.00	0.0
4	0.0	0.89	0.01	1.1	0.90	0.00	0.0
5	0.0	0.89	0.01	1.1	0.90	0.00	0.0
7.5	1.1	0.89	0.01	1.1	0.89	0.01	1.1
10	1.1	0.89	0.01	1.1	0.88	0.02	2.2
15	2.2	0.89	0.01	1.1	0.88	0.02	2.2
20	2.2	0.88	0.02	2.2	0.88	0.02	2.2
25	2.2	0.88	0.02	2.2	0.87	0.03	3.3
30	3.3	0.87	0.03	3.3	0.87	0.03	3.3
45	4.4	0.87	0.03	3.3	0.86	0.04	4.4
60	4.4	0.86	0.04	4.4	0.86	0.04	4.4
75	5.6	0.85	0.05	5.6	0.85	0.05	5.6
90	5.6	0.84	0.06	6.7	0.85	0.05	5.6
105	6.7	0.84	0.06	6.7	0.85	0.05	5.6
120	6.7	0.83	0.07	7.8	0.84	0.06	6.7

APPENDIX 4:

(a) Experiments D1 to D5: Variation of weight with time

time (min)	Sample weight (gram)				
	D1	D2	D3	D4	D 5
0	0.90	0.90	0.90	0.90	0.90
1	0.90	0.89	0.90	0.90	0.90
2	0.90	0.88	0.90	0.89	0.90
3	0.90	0.87	0.90	0.89	0.90
4	0.90	0.86	0.90	0.88	0.90
5	0.90	0.85	0.90	0.88	0.90
7.5	0.90	0.84	0.90	0.87	0.90
10	0.89	0.83	0.90	0.87	0.89
15	0.89	0.81	0.89	0.87	0.89
20	0.88	0.81	0.89	0.84	0.89
25	0.88	0.79	0.89	0.84	0.88
30	0.88	0.79	0.89	0.83	0.88
45	0.87	0.77	0.88	0.81	0.88
60	0.86	0.77	0.88	0.80	0.87
75	0.86	0.76	0.87	0.80	0.87
90	0.86	0.76	0.87	0.79	0.87
105	0.86	0.76	0.86	0.79	0.86
120	0.85	0.76	0.86	0.79	0.86

(b) Experiments D1 to D5: Relative cumulative weight loss data

Time (Min)	Relative cumulative weight loss $\frac{\Delta W_t}{W_o} (\%)$				
	D1	D2	D3	D4	D5
0	0.0	0.0	0.0	0.0	0.0
1	0.0	1.1	0.0	0.0	0.0
2	0.0	2.2	0.0	1.1	0.0
3	0.0	3.3	0.0	1.1	0.0
4	0.0	4.4	0.0	2.2	0.0
5	0.0	5.6	0.0	2.2	0.0
7.5	0.0	6.7	0.0	3.3	0.0
10	1.1	7.8	0.0	3.3	1.1
15	1.1	10.0	1.1	3.3	1.1
20	2.2	10.0	1.1	6.7	1.1
25	2.2	12.2	1.1	6.7	2.2
30	2.2	12.2	1.1	7.8	2.2
45	3.3	14.4	2.2	10.0	2.2
60	4.4	14.4	2.2	11.1	3.3
75	4.4	15.6	3.3	11.1	3.3
90	4.4	15.6	3.3	12.2	3.3
105	4.4	15.6	4.4	12.2	4.4
120	5.6	15.6	4.4	12.2	4.4

APPENDIX 5:

(a) Experiments E1 to E6: Sample weight change with time

Time (Min)	Sample weight (gram)					
	E1	E2	E3	E4	E5	E6
0	0.90	0.90	0.90	0.90	0.90	0.90
1	0.90	0.90	0.90	0.90	0.89	0.89
2	0.90	0.90	0.90	0.90	0.88	0.87
3	0.90	0.90	0.90	0.89	0.87	0.86
4	0.90	0.90	0.90	0.89	0.86	0.86
5	0.90	0.90	0.90	0.89	0.85	0.85
7.5	0.90	0.90	0.89	0.88	0.84	0.84
10	0.90	0.90	0.89	0.88	0.83	0.83
15	0.90	0.89	0.89	0.87	0.82	0.81
20	0.90	0.89	0.89	0.86	0.81	0.80
25	0.90	0.89	0.88	0.85	0.80	0.79
30	0.90	0.89	0.88	0.85	0.79	0.79
45	0.90	0.88	0.87	0.83	0.78	0.77
60	0.90	0.88	0.86	0.82	0.76	0.76
75	0.89	0.87	0.86	0.81	0.76	0.75
90	0.89	0.87	0.85	0.80	0.75	0.75
105	0.89	0.86	0.85	0.80	0.75	0.75
120	0.89	0.86	0.85	0.78	0.75	0.75
150	0.89	0.85	0.84			
180	0.89	0.84	0.83			
210	0.89	0.84	0.83			
240	0.88	0.84	0.83			

(b) Experiments E1 to E6: Relative cumulative weight loss data

Time (Min)	Relative cumulative weight loss, $\frac{\Delta W_t}{W_o}$ (%)					
	E1	E2	E3	E4	E5	E6
0	0.0	0.0	0.0	0.0	0.0	0.0
1	0.0	0.0	0.0	0.0	1.1	1.1
2	0.0	0.0	0.0	0.0	2.2	3.3
3	0.0	0.0	0.0	1.1	3.3	4.4
4	0.0	0.0	0.0	1.1	4.4	4.4
5	0.0	0.0	0.0	1.1	5.6	5.6
7.5	0.0	0.0	1.1	2.2	6.7	6.7
10	0.0	0.0	1.1	2.2	7.8	7.8
15	0.0	1.1	1.1	3.3	8.9	10.0
20	0.0	1.1	1.1	4.4	10.0	11.1
25	0.0	1.1	2.2	5.6	11.1	12.2
30	0.0	1.1	2.2	5.6	12.2	12.2
45	0.0	2.2	3.3	7.8	13.3	14.4
60	0.0	2.2	4.4	8.9	15.6	15.6
75	1.1	3.3	4.4	10.0	15.6	16.7
90	1.1	3.3	5.6	11.1	16.7	16.7
105	1.1	4.4	5.6	11.1	16.7	16.7
120	1.1	4.4	5.6	13.3	16.7	16.7
150	1.1	5.6	6.7			
180	1.1	6.7	6.7			
210	1.1	6.7	6.7			
240	2.2	6.7	6.7			

# APPENDIX 6

## Data on porosity experiments

Time (Min)	F1 = E5		F2		F3	
	$W_t$ (g)	$\frac{\Delta W_t}{W_o}$ (%)	$W_t$ (g)	$\frac{\Delta W_t}{W_o}$ (%)	$W_t$ (g)	$\frac{\Delta W_t}{W_o}$ (%)
0	0.90	0.0	1.02	0.0	1.14	0.0
1	0.89	1.1	1.01	1.0	1.13	0.9
2	0.88	2.2	1.00	2.0	1.12	1.8
3	0.87	3.3	1.00	2.0	1.11	2.6
4	0.86	4.4	0.99	2.9	1.10	3.5
5	0.85	5.6	0.97	4.9	1.09	4.4
7.5	0.84	6.7	0.97	4.9	1.09	4.4
10	0.83	7.8	0.96	5.9	1.08	5.3
15	0.82	8.9	0.94	7.8	1.06	7.0
20	0.81	10.0	0.93	8.8	1.05	7.9
25	0.80	11.1	0.92	9.8	1.04	8.8
30	0.79	12.2	0.91	10.8	1.03	9.6
45	0.78	13.3	0.88	13.7	1.00	12.3
60	0.76	15.6	0.87	14.7	0.99	13.2
75	0.76	15.6	0.86	15.7	0.98	14.0
90	0.75	16.7	0.86	15.7	0.98	14.0
105	0.75	16.7	0.86	15.7	0.98	14.0
120	0.75	16.7				



# APPENDIX 7

## Effect of lime addition

Reaction time (Min)	G1		G2		G3	
	$W_t(g)$	$\frac{\Delta W_t}{W_o} (\%)$	$W_t(g)$	$\frac{\Delta W_t}{W_o} (\%)$	$W_t(g)$	$\frac{\Delta W_t}{W_o} (\%)$
0	0.90	0.0	0.90	0.0	0.90	0.0
1	0.90	0.0	0.89	1.1	0.89	1.1
2	0.90	0.0	0.88	2.2	0.89	1.1
3	0.90	0.0	0.88	2.2	0.89	1.1
4	0.90	0.0	0.87	3.3	0.88	2.2
5	0.90	0.0	0.86	4.4	0.88	2.2
7.5	0.89	1.1	0.86	4.4	0.87	3.3
10	0.89	1.1	0.85	5.6	0.86	4.4
15	0.89	1.1	0.83	7.8	0.85	5.6
20	0.89	1.1	0.82	8.9	6.84	6.7
25	0.88	2.2	0.81	10.0	0.83	7.8
30	0.88	2.2	0.80	11.1	0.82	8.9
45	0.87	3.3	0.78	13.3	0.80	11.1
60	0.87	3.3	0.77	14.4	0.79	12.2
75	0.87	3.3	0.76	15.6	0.78	13.3
90	0.86	4.4	0.75	16.7	0.77	14.4
105	0.86	4.4	0.75	16.7	0.77	14.4
120	0.86	4.4				

# APPENDIX 8

CO<sub>2</sub>/CO content of exit gas

Expt. No.	Reading No.	Volume CO <sub>2</sub> V <sub>CO<sub>2</sub></sub> (cm <sup>3</sup> )	Volume CO V <sub>CO</sub> (cm <sup>3</sup> )	$\frac{V_{CO_2}}{V_{CO}}$	Average $V_{CO_2}/V_{CO}$	Average $P_{CO_2}/P_{CO}$
B3	A	1.2	0.8	1.50	1.47	2.33
	B	1.9	1.3	1.46		
	C	3.5	2.4	1.46		
	D	2.8	1.9	1.47		
B4	A	3.1	2.4	1.29	1.38	2.19
	B	2.5	1.9	1.32		
	C	5.1	3.6	1.42		
	D	2.1	1.4	1.50		
B5	A	2.0	1.7	1.18	1.13	1.78
	B	1.7	1.5	1.13		
	C	1.2	1.1	1.09		
B6	A	2.4	2.2	1.09	1.06	1.68
	B	0.9	0.9	1.00		
	C	1.4	1.3	1.08		
	D	2.9	2.7	1.07		
B7	A	2.3	3.2	0.72	0.75	1.18
	B	1.8	2.3	0.78		

Expt No.	Reading No.	Volume CO <sub>2</sub> $V_{CO_2}$ (cm <sup>3</sup> )	Volume CO $V_{CO}$ (cm <sup>3</sup> )	$\frac{V_{CO_2}}{V_{CO}}$	Average $V_{CO_2}/V_{CO}$	Average $P_{CO_2}/P_{CO}$
E1	E	7.0	4.1	1.71	1.71	2.71
E2	C	3.3	2.0	1.65	1.67	2.64
	D	2.1	1.3	1.62		
	E	1.4	0.8	1.75		
E3	C	1.7	1.1	1.55	1.53	2.42
	D	2.5	1.7	1.47		
	E	1.9	1.3	1.46		
E4	A	1.5	1.1	1.36	1.50	2.37
	B	2.4	1.6	1.50		
	C	1.8	1.1	1.64		
	D	1.2	0.8	1.50		
E5	A	3.1	2.1	1.48	1.44	2.28
	B	2.0	1.4	1.43		
	C	2.4	1.7	1.41		
	D	1.7	1.2	1.42		
E6	A	1.3	0.9	1.44	1.42	2.25
	B	1.9	1.4	1.36		
	C	1.6	1.1	1.45		
	D	1.7	1.2	1.43		

(i) Conversion of volume ratios to  $P_{CO_2}/P_{CO}$  was effected by the relation

$$\frac{P_{CO_2}}{P_{CO}} = \frac{V_{CO_2}}{V_{CO}} \times \frac{\text{density CO}_2 \text{ at temperature, } T}{\text{density CO at the same temp.}}$$

(ii) The readings were taken as follows:

Reading (A) was taken 10 minutes from commencement of the reaction in experiments to monitor continuous weight loss. Readings (B), (C), (D) and (E) were taken 5, 20, 60 and 180 minutes respectively from commencement of the perfectly sealed experiments. Time of commencement in this case, is relative to that of the very first interval.

APPENDIX 9

Data for the kinetic analysis of temperature effect

(a) Sample weight loss with time

Reaction time (min)	Sample weight loss, $\Delta W_t$ (grams)					
	E1	E2	E3	E4	E5	E6
0	0.00	0.00	0.00	0.00	0.00	0.00
1	"	"	"	"	0.01	0.01
2	"	"	"	"	0.02	0.03
3	"	"	"	0.01	0.03	0.04
4	"	"	"	0.01	0.04	0.04
5	"	"	"	0.01	0.05	0.05
7.5	"	"	0.01	0.02	0.06	0.06
10	"	"	0.01	0.02	0.07	0.07
15	"	0.01	0.01	0.03	0.08	0.09
20	"	0.01	0.01	0.04	0.09	0.10
25	"	0.01	0.02	0.05	0.10	0.11
30	"	0.01	0.02	0.05	0.11	0.11
45	"	0.02	0.03	0.07	0.12	0.13
60	"	0.02	0.04	0.08	0.14	0.14
75	0.01	0.03	0.04	0.09	0.14	0.15
90	0.01	0.03	0.05	0.10	0.15	0.15
105	0.01	0.04	0.05	0.10	0.15	0.15
120	0.01	0.04	0.05	0.12	0.15	0.15
150	0.01	0.05	0.06			
180	0.01	0.06	0.07			
210	0.01	0.06	0.07			

(b) Carbon loss as a function of time and temperature

Time (min)	Weight of carbon reacted, $W_t^C$ (grams)					
	E1	E2	E3	E4	E5	E6
0	0.00	0.00	0.00	0.00	0.00	0.00
1	"	"	"	"	0.0032	0.0032
2	"	"	"	"	0.0064	0.0096
3	"	"	"	0.0032	0.0096	0.0128
4	"	"	"	0.0032	0.0128	0.0128
5	"	"	"	0.0032	0.0160	0.0161
7.5	"	"	0.0032	0.0064	0.0192	0.0193
10	"	"	0.0032	0.0064	0.0224	0.0225
15	"	0.0032	0.0032	0.0096	0.0256	0.0289
20	"	0.0032	0.0032	0.0128	0.0289	0.0321
25	"	0.0032	0.0064	0.0160	0.0322	0.0353
30	"	0.0032	0.0064	0.0160	0.0353	0.0353
45	"	0.0063	0.0096	0.0224	0.0385	0.0417
60	"	0.0063	0.0127	0.0255	0.0449	0.0449
75	0.00315	0.0095	0.0127	0.0287	0.0479	0.0471
90	0.00315	0.0095	0.0159	0.0319	0.0471	0.0471
105	0.00315	0.0126	0.0159	0.0319	0.0471	0.0471
120	0.00315	0.0126	0.0159	0.0383	0.0471	0.0471
150	0.00315	0.0158	0.0191			
180	0.00315	0.0190	0.0223			
210	0.00315	0.0190	0.0223			
240	0.00630	0.0190	0.0223			

(c) Unreacted carbon in the sample as a function of time and temperature

Reaction time (min)	$W_t^c$ , Weight of unreacted carbon (gram)					
	E1	E2	E3	E4	E5	E6
0	0.0471	0.0471	0.0471	0.0471	0.0471	0.0471
1	"	"	"	0.0471	0.0439	0.0439
2	"	"	"	0.0471	0.0407	0.0375
3	"	"	"	0.0439	0.0375	0.0343
4	"	"	"	0.0439	0.0343	0.0343
5	"	"	"	0.0439	0.0311	0.0310
7.5	"	"	0.0439	0.0407	0.0273	0.0278
10	"	"	0.0439	0.0407	0.0247	0.0246
15	"	0.0439	0.0439	0.0375	0.0215	0.0182
20	"	0.0439	0.0439	0.0343	0.0182	0.0150
25	"	0.0439	0.0407	0.0311	0.0150	0.0118
30	"	0.0439	0.0407	0.0311	0.0118	0.0118
45	"	0.0408	0.0375	0.0247	0.0086	0.0054
60	"	0.0408	0.0344	0.0216	0.0022	0.0022
75	0.04395	0.0376	0.0344	0.0184	0.0022	0.0000
90	0.04395	0.0376	0.0312	0.0152	0.0000	0.0000
105	0.04395	0.0345	0.0312	0.0152	0.0000	0.0000
120	0.04395	0.0345	0.0312	0.0088	0.0000	0.0000
150	0.04395	0.0313	0.0280			
180	0.04395	0.0281	0.0248			
210	0.04395	0.0281	0.0248			
240	0.0408	0.0281	0.0248			

$$W_t^c = W_0^c - \Delta W_t^c = 0.0471 - \Delta W_t^c$$

(d) Initial carbon amount as a fraction of unreacted carbon.  
Time-temperature dependence

Reaction time (min)	$w_o^c/w_t^c$ as a percentage					
	E1	E2	E3	E4	E5	E6
0	1.000	1.000	1.000	1.000	1.000	1.000
1	"	"	"	1.000	1.072	1.072
2	"	"	"	1.000	1.157	1.256
3	"	"	"	1.072	1.256	1.373
4	"	"	"	1.072	1.373	1.373
5	"	"	"	1.072	1.514	1.519
7.5	"	"	1.073	1.157	1.725	1.694
10	"	"	1.073	1.157	1.907	1.915
15	"	1.072	1.073	1.256	2.191	2.588
20	"	1.072	1.073	1.373	2.588	3.140
25	"	1.072	1.157	1.514	3.140	3.992
30	"	1.072	1.157	1.514	3.992	3.992
45	"	1.154	1.256	1.907	5.477	8.722
60	"	1.154	1.369	2.181	21.41	21.41
75	1.072	1.253	1.369	2.560	21.41	$\infty$
90	1.072	1.253	1.510	3.099	$\infty$	$\infty$
105	1.072	1.365	1.510	3.099	$\infty$	$\infty$
120	1.072	1.365	1.510	5.352	$\infty$	$\infty$
150	1.072	1.505	1.682			
180	1.072	1.676	1.899			
210	1.072	1.676	1.899			
240	1.154	1.676	1.899			



APPENDIX 10

(a) Derivation of equation 14: Extent of carbon burn-off

- (i) If from gas analysis,  $P_{CO_2}/P_{CO} = \alpha$   
the weights of  $CO_2$  and  $CO$  gases evolved are  
related by:

$$W_{CO_2} = \alpha W_{CO} \dots\dots\dots (a)$$

- (ii) If the total weight loss at time (t) is  $\Delta W_t$ ,

$$\Delta W_t = W_{CO_2} + W_{CO}$$

i.e.  $\Delta W_t = \alpha W_{CO} + W_{CO}$

or  $W_{CO} = \frac{\Delta W_t}{1 + \alpha} \dots\dots\dots (b)$

- (iii) From the stoichiometry of the equation



per gram  $CO_2$  evolved, carbon reacted =  $\frac{12}{44}$  g

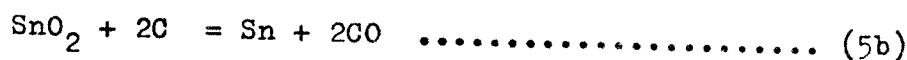
= 0.273 g

$\therefore$  If at time (t) carbon dioxide evolved =  $W_{CO_2}$  g

carbon reacted =  $0.273 W_{CO_2}$

=  $0.273 \alpha W_{CO}$  (From (a))

- (iv) Similarly, from the equation



when at time (t) carbon monoxide evolved =  $W_{CO}$  g

carbon reacted =  $\frac{24}{56} W_{CO} = 0.429 W_{CO}$

(v) i.e At time (t),

$$\text{total carbon reacted } \Delta W_t^C = 0.273 \alpha W_{CO} + 0.429 W_{CO}$$

$$\Delta W_t^C = W_{CO}(0.273\alpha + 0.429)$$

$$\text{or from (b), } \Delta W_t^C = \frac{\Delta W_t}{1 + \alpha} (0.273\alpha + 0.429)$$

(b) Derivation of equation (18): calculated amount of tin produced.

(i) From the stoichimetry of equation (4b) as shown in appendix, 10a ,

the reaction of 12g carbon would produce 118.69 g Sn

∴ For  $0.273 \alpha W_{CO}$  of carbon reacted,

$$\text{amount tin produced} = 2.697 \alpha W_{CO} \text{ g}$$

(ii) Similarly from equation (5b) of the previous appendix,

When  $0.429 W_{CO}$  g carbon has reacted,

$$\text{amount tin produced} = 2.119 W_{CO} \text{ g}$$

(iii) ∴ At time (t), amount of tin produced

$$= 2.697 \alpha W_{CO} + 2.119 W_{CO}$$

$$= W_{CO} (2.697 \alpha + 2.119)$$

$$= \frac{\Delta W_t}{1 + \alpha} (2.697 \alpha + 2.119)$$

(iv) At the end of the experiment,

$$\Delta W_t = \Delta W$$

∴ Weight of tin produced

$$W_{Sn} = \frac{\Delta W}{1 + \alpha} (2.697 \alpha + 2.119) \dots \dots \dots (18)$$

# APPENDIX 11

## Reduction of cassiterite concentrate by carbon monoxide:

### Sample calculations

#### (a) Conversion of pH to $H^+$ concentration ( $C_{H^+}$ )

$$- \log C_{H^+} = pH - \frac{A Z_{H^+}^2 \sqrt{I}}{1 + B_{\pm} \sqrt{I}}$$

$$Z_{H^+} = 1$$

$$\bar{a} = 5 \text{ \AA}$$

For 0.005 molar KOH solution, the ionic strength  $I = \frac{1}{2} (0.005(+1)^2 + 0.005 (-1)^2)$   
 $= 0.005$

At  $20^\circ\text{C}$ ,

$$A = 0.5070, \text{ for } \bar{a} \text{ in angstrom}$$

$$B = 0.3282$$

$$\therefore - \log C_{H^+} = pH - \frac{0.51 \sqrt{0.005}}{1 + 1.64 \sqrt{0.005}}$$

$$- \log C_{H^+} = pH - 0.032$$

#### (b) Calculation of $OH^-$ concentration ( $C_{OH^-}$ )

from corresponding  $C_{H^+}$  values

At  $20^\circ\text{C}$ , the ionic product of water

$$C_{H^+} \times C_{OH^-} = 10^{-14.17}$$

$$\therefore \log C_{OH^-} = -14.17 - \log C_{H^+}$$

$$C_{OH^-} = \text{antilog} (-14.17 - \log C_{H^+})$$

- (c) Evaluation of g-moles  $\text{OH}^-$  contained in the KOH solution at any time,  $t$ .

$$\text{g-moles } \text{OH}^- = C_{\text{OH}^-} \left( \frac{\text{g-mol}}{\text{litre}} \right) \times V \text{ (litre)}$$

where:  $V$  = volume of the KOH solution  
 = 0.150 litre.

- (d) Calculation of g-moles  $\text{OH}^-$  reacted, the corresponding Sn amount formed and  $\text{Sn}_t/\text{Sn}_f$  ratio.

- (i) At the start of the experiments the pH of the KOH solution was 11.9. By using the calculations shown above,  
 g-moles  $\text{OH}^-$  contained =  $0.79 \times 10^{-3}$ .

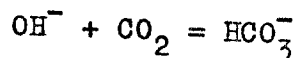
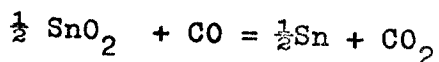
If at time ( $t$ ) in the course of the experiment the pH decreased to , for example, 11.5 the g-moles  $\text{OH}^-$  contained in the KOH solution would be calculated in a similar manner as  $0.30 \times 10^{-3}$ .

i.e  $\text{OH}^-$  reacted in time interval ( $t$ ),

$$= (0.75 - 0.30) \times 10^{-3} \text{ g-mole}$$

$$= 0.45 \times 10^{-3} \text{ g-mole.}$$

- (ii) From the stoichiometry of the reactions



For every g-mole  $\text{OH}^-$  reacted,  $\frac{1}{2}$  a g-mole Sn is formed assuming complete  $\text{CO}_2$  absorption and  $\text{HCO}_3^-$  stability.

∴ For the above example, at time ( $t$ ),

$$\text{g-moles Sn formed} = \frac{0.45}{2} \times 10^{-3}$$

$$\begin{aligned} \text{Weight of Sn formed } \text{Sn}_t &= \frac{0.45}{2} \times 10^{-3} \times 118.69 \text{ g} \\ &= 26.71 \text{ mg} \end{aligned}$$

(iii) At the end of the experiments,

KOH solution pH = 10.0

By calculation,  $C_{OH^-} = 0.06 \times 10^{-3}$  g-mole/litre

contained  $OH^-$  =  $0.007 \times 10^{-3}$  g-mole

reacted  $OH^-$  =  $0.741 \times 10^{-3}$  g-mole

Sn formed =  $0. \frac{741}{2} \times 10^{-3}$  g-mole

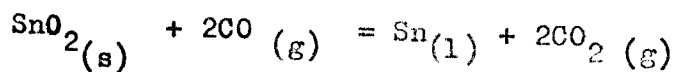
Weight Sn formed  $Sn_f = 0. \frac{741}{2} \times 10^{-3} \times 118.69$

= 45.97 mg

APPENDIX 12

Calculation of tin content of reacted samples from  
sample weight loss data

Considering the reaction



and in the absence of volatile matter in the cassiterite concentrate, the weight loss of the reacted sample corresponds to the oxygen lost.

Loss of 32g oxygen leads to formation of 118.69g Sn

∴ For a loss of (y) mg oxygen,

$$\text{Amount of tin formed} = \frac{118.69}{32} y \text{ mg.}$$